Pesquisas em Geociências

v. 50, nº 2 (2023)
doi.org/10.22456/1807-9806.131140

Artigo de Pesquisa

Wind-blown continental dust as a fuel for paleoproductivity along the southwestern Atlantic Ocean during the last glacial period

Poeira continental soprada pelo vento como combustível para paleoprodutividade ao longo do sudoeste do Oceano Atlântico durante o último período glacial

Renato Pereira LOPES[1], Márcio Silva de SOUZA[2]

[1]Av. Rio Grande, 45, Caixa Postal 15, Cassino, Rio Grande - RS, Brazil. paleonto_furg@yahoo.com.br (corresponding author).

[2]Universidade Federal de Pelotas, Instituto de Biologia, Departamento de Botânica. Campus Capão do Leão s/n, 96160-000 Capão do Leão-RS, Brazil. souzamsd@gmail.com

Abstract: Glaciogenic dust has a strong relationship with global climate and ocean biogeochemical processes especially during glacial periods, being a major source of nutrients, mainly iron, that increase marine productivity. Different studies have attributed higher marine paleoproductivity along the southwestern Atlantic during the last glacial period to fluvial inputs and upwelling, but the possible influence of continental dust on that process is still unknown. This paper presents evidence suggesting that eolian-sourced glaciogenic dust favored higher ocean productivity during the last glacial, recorded in three sediment cores obtained on the lower continental slope off southern Brazil (~29°-30°S, ~47°W) at water depths between 1,514 and 2,091 m. The sampled sediments are silt-dominated terrigenous siliciclastics, but higher proportions of sand-sized biogenic carbonate (mostly foraminifer tests) at intervals corresponding to the stadials MIS 4 and 2 and parts of the interstadial MIS 3 point to intervals of increased productivity, correlated with pulses of higher deflation of dust from southern South America as recorded in the EPICA Dome C ice core in Antarctica. It is proposed that glacial climate-driven increased eolian processes transported iron-bearing dust produced by the expanded Patagonian ice sheet up to the southwestern Atlantic, fueling higher phytoplankton productivity and thus favoring the proliferation of planktonic and benthic foraminifera recorded in the cores. Eventual anthropogenically-driven reduction of tropical-sourced summer rainfall reaching southern South America, driven by equatorial ocean warming and deforestation in the Amazon region, may increase dust deflation and thus affect ocean productivity along the southwestern Atlantic in the future.

Keywords: Eolian processes, Glaciogenic dust, Loess, Paleoclimate, Marine Geology, Paleoceanography

Recebido: 03/2023
Aceito: 08/2023
Publicado: 08/2023

Resumo: A poeira glaciogênica tem forte relação com o clima global e os processos biogeoquímicos oceânicos, principalmente durante os períodos glaciais, sendo uma importante fonte de nutrientes, como o ferro, que aumentam a produtividade marinha. Diferentes estudos tenham atribuído a maior paleoprodutividade marinha ao longo do Atlântico sudoeste durante o último período glacial a aportes fluviais e ressurgência, mas a possível influência da poeira continental nesse processo ainda é desconhecida. Este artigo apresenta evidências sugerindo que a poeira glaciogênica de origem eólica favoreceu maior produtividade oceânica durante a última glaciação, registrada em três testemunhos sedimentares obtidos no talude continental inferior no sul do Brasil (~29°-30°S, ~47°W) em profundidades da lâmina d'água entre 1.514 e 2.091 m. Os sedimentos amostrados são siliciclásticos terrígenos dominados por silte, mas maiores proporções de carbonato biogênico de tamanho areia (principalmente testes de foraminíferos) em intervalos correspondentes aos estadiais MIS 4 e 2 e partes do interestadial MIS 3 indicam intervalos de maior produtividade, correlacionados com pulsos de maior deflação de poeira do sul da América do Sul, conforme registrado no testemunho de gelo antártico obtido no EPICA Domo C. Propõe-se que os processos eólicos intensificados devido ao clima glacial transportaram para o Atlântico sudoeste poeira contendo ferro produzida pela expansão do manto de gelo da Patagônia, alimentando uma maior produtividade do fitoplâncton eassim favorecendo a proliferação de foraminíferos planctônicos e bentônicos registrados nos testemunhos. A eventual redução antrópica das chuvas de verão de origem tropical que atingem o sul da América do Sul, impulsionada pelo aquecimento do oceano equatorial e pelo desmatamento na região amazônica, pode aumentar a deflação de poeira, assim afetar a produtividade do oceano ao longo do Atlântico sudoeste no futuro.

Palavras-chave: Processos eólicos, Poeira glaciogênica, *Loess*, Paleoclima, Geologia Marinha, Paleoceanografia

1. Introduction

On October 25th, 2021, a large dust cloud was observed over northern Uruguay-southern Brazil, stretching over the continent and adjacent southwestern Atlantic Ocean (Fig. 1A). The dust cloud was produced by an intense windstorm that swept across the Neuquén Province, in central-western Argentina (CWA), resuspending and entraining large amounts of silt-sized dust particles. The dust was deflated from Quaternary deposits that cover large areas across the lowlands east of the Andes occupied by arid and semiarid environments within the Arid Diagonal of South America (Bruniard, 1982). Although such extreme events capable of carrying significant amounts of dust up to southern Brazil are not common today (Gassó & Torres, 2019), different records indicate more frequent and intense eolian deflation and transport in the past, especially during colder phases (stadials) of glacial periods (Clapperton, 1993; Zárate & Tripaldi, 2012).

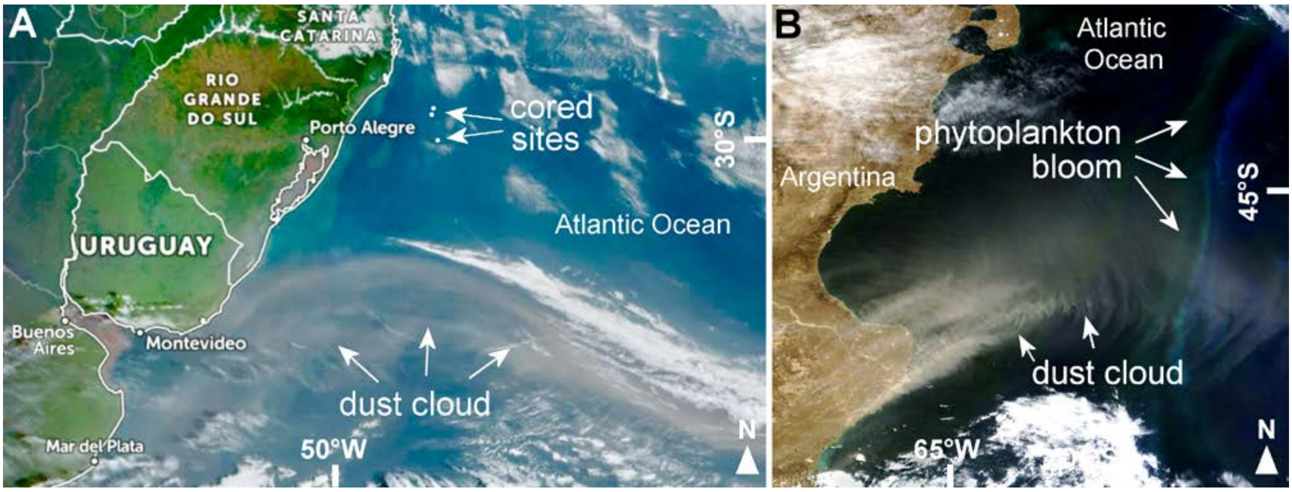

Figure 1. A - Zoom Earth (https://zoom.earth) image showing the Patagonian dust cloud carried by southwesterly winds over the southwestern Atlantic off Uruguay and southern Brazil on October 25th, 2021, the location of the cores described in the text is indicated. B - Aqua MODIS image from the Terra satellite taken on January 14, 2010, showing a phytoplankton bloom in the South Atlantic off the coast of Argentina produced by wind-blown dust from Patagonia (https://earthobservatory.nasa.gov/images/42446/patagonian-dust-over-the-atlantic-ocean).

Figura 1. A - Imagem Zoom Earth (https://zoom.earth) mostrando a nuvem de poeira da Patagônia transportada por ventos de sudoeste sobre o Atlântico sudoeste ao largo do Uruguai e sul do Brasil em 25 de outubro de 2021, a localização dos testemunhos descritos no texto está indicada. B - Imagem Aqua MODIS do satélite Terra tirada em 14 de janeiro de 2010 mostrando uma floração de fitoplâncton no Atlântico Sul, na costa da Argentina, produzida por poeira da Patagônia transportada pelo vento (https://earthobservatory.nasa.gov/images/42446/patagonian-dust-over-the-atlantic-ocean).

During glacial periods, wind-blown dust from the major sources of South America, located on the Puna-Altiplano Plateau (PAP, 15º-22ºS), CWA (27º-35ºS) and northern Patagonia (39º-52ºS), reached up to East Antarctica (Prospero *et al.,* 2002; Gaiero, 2007; Lambert *et al.,* 2008; 2012; Weber *et al.,* 2012; Gili *et al.,* 2017). Together with volcanic ash, this dust has been identified as a major source of bioavailable macronutrients (iron, nitrate and silica) to the South Atlantic and Atlantic sector of the Southern Ocean (Kumar *et al.,* 1995; Gaiero *et al.,* 2003; Johnson *et al.,* 2011; Noble *et al.,* 2012; Martínez-García *et al.,* 2014; Paparazzo *et al.,* 2018; Shoenfelt *et al.,* 2018). These ocean waters are characterized as high nitrate low chlorophyll (HNLC) because primary productivity is limited today by the deficiency in bioavailable iron, which is essential for the phytoplankton (mainly diatoms) to utilize the nitrate and phosphate in surface waters for synthesizing chlorophyll (Martin, 1990). On the other hand, the iron contained in eolian-sourced dust had contributed to episodic increases in phytoplankton productivity in the South Atlantic (Fig. 1B) and Southern Ocean since the Mid-Pleistocene Transition (MPT) around 1.25 Ma ago, which has been a major contribution for maintaining the levels of atmospheric carbon dioxide (CO_{2atm}) at the pre-industrial levels of ~200 ppmv during glacial periods through the 'biological pump', i.e., the removal of CO_{2atm} as a result of higher phytoplankton productivity (Martin, 1990; Maher *et al.,* 2010; Martínez-García *et al.,* 2011).

The dust sourced from Patagonia and CWA to the South Atlantic-Austral Ocean and Antarctica had been generated by the glaciers of the Patagonian ice sheet that expanded during glacial periods covering the central-southern Andes (Clapperton, 1993; Hulton *et al.,* 1994; Iriondo, 1997; Zárate 2006). That dust was also transported northeastward up to the Pampean Region of Argentina, where it accumulated as a loess belt around the Pampean Sand Sea, which together form the Pampean Eolian System (Iriondo & Kröhling, 1995; Zárate & Tripaldi, 2012). The dust from the PAP was carried southeastwards by the subtropical jet (STJ), which is stronger during winter, especially under conditions of El Niño, and capable of transporting large quantities of dust across southern Bolivia, Paraguay, Uruguay, southern Brazil, and northern Argentina (Gaiero *et al.,* 2013; Torre *et al.,* 2019).

The dust deflated from the PAP, piedmont deposits west of the Andes and the Pampean Eolian System reached Uruguay and the state of Rio Grande do Sul in southern Brazil as indicated by loess deposits (Panario & Gutiérrez, 1999; Lopes *et al.*, 2016a). The presence of these deposits implies that the wind-blown dust may have reached lower latitudes along the Southwestern Atlantic as well, where it may have contributed to increased productivity (as shown in Figure 1B). Sedimentological data obtained from the deep-sea core SIS-249 retrieved from the lower continental slope off the southern Brazilian continental margin indicate higher accumulation rates and increased sand-sized biogenic carbonate inputs during the stadial Marine Isotope Stage (MIS) 4, which could have resulted from higher ocean productivity driven by increased eolian inputs (Lopes *et al.,* 2021a).

Increases in paleoproductivity during the last glacial recorded on other deep-sea cores obtained off southern Brazil have been attributed to inputs of nutrient-rich sediments sourced by fluvial systems reaching the coast and upwelling of nutrient-rich water masses, but the possible influence of glaciogenic dust has not been discussed in detail. In this paper, this possibility is further explored by comparing sedimentological data from SIS-249 with two other cores collected nearby that encompass the latest Pleistocene-earliest Holocene (MIS 3 to MIS 1) interval (Frozza *et al.,* 2020; Petró *et al.,* 2021; Suárez-Ibarra *et al.,* 2022). The numerical ages mentioned here obtained through luminescence or other methods are expressed as b2k (before 2000 AD), whereas radiocarbon ages are expressed as years BP relative to 1950 AD. Climatic stages (MIS) are expressed according to Railsback *et al.* (2015) and stage boundaries are defined according to the LR04 benthic stack (Lisiecki & Raymo, 2005).

2. Study Area

2.1 Geological Setting

The analysis presented here is based on three cores obtained as part of a project aimed at investigating the paleoproductivity during the late Pleistocene-Holocene within the scope of the International Ocean Drilling Program (IODP). The cores were collected at ~29°-30°S/~47°W in the southern Brazilian margin off the northern coast of Rio Grande do Sul state (Fig. 2A) at water depths of 1,514 m (SIS-188), 1,514 m (SAT-048A) and 2,091 m (SIS-249), downslope of the Rio Grande Terrace (RGT). The Brazilian margin is formed of siliciclastic terrigenous sediments accumulated after the opening of the South Atlantic in the Cretaceous, which led to the development of several marginal sedimentary basins, including the Pelotas Basin in the study area (Asmus and Ponte, 1973; Barboza *et al.* 2021a). The mineralogy of the sediments accumulated on the slope off Rio Grande do Sul indicates these were sourced from the adjacent coastal plain, and are derived from igneous, sedimentary, and metamorphic rocks of the Sul-rio-grandense Shield, Paraná Basin, and the Andes (Lopes *et al.,* 2021a; Carassai *et al.,* 2019; Chemale Jr. *et al.,* 2021).

The shelf break at the study area is located at a water depth of ~200 m and the upper slope is narrow and transitions to the RGT (Fig. 2B). This geomorphological feature is located at water depths between 200 and 500 m and exhibits a flat upper surface formed of consolidated sand with polymetallic nodules, whereas its flanks are dominated by silt at depths of ≥500 m (Lisniowski & Alves, 2018a,b; Alves *et al.,* 2021). Erosive processes on the RGT are indicated by longitudinal furrows and escarpments on its surface probably produced by water currents, whereas gullies along its flanks indicate downslope mass movements, which may have been triggered by sea-level oscillations and methane degassing as indicated by pockmarks (Lisniowski & Alves 2018a,b; Lopes *et al.,* 2021a). The slope is composed mainly of terrigenous silt, transferred from the shelf through downslope mass movements (Butler, 1970; Zembruscki, 1979; Lopes *et al.,* 2021a), although deep contour currents could have influenced sediment accumulation through lateral transport along the bottom (Alves *et al.,* 2021). The carbonate content is relatively low, and the sand fraction is dominated by tests of foraminifers (Kowsmann *et al.,* 1977).

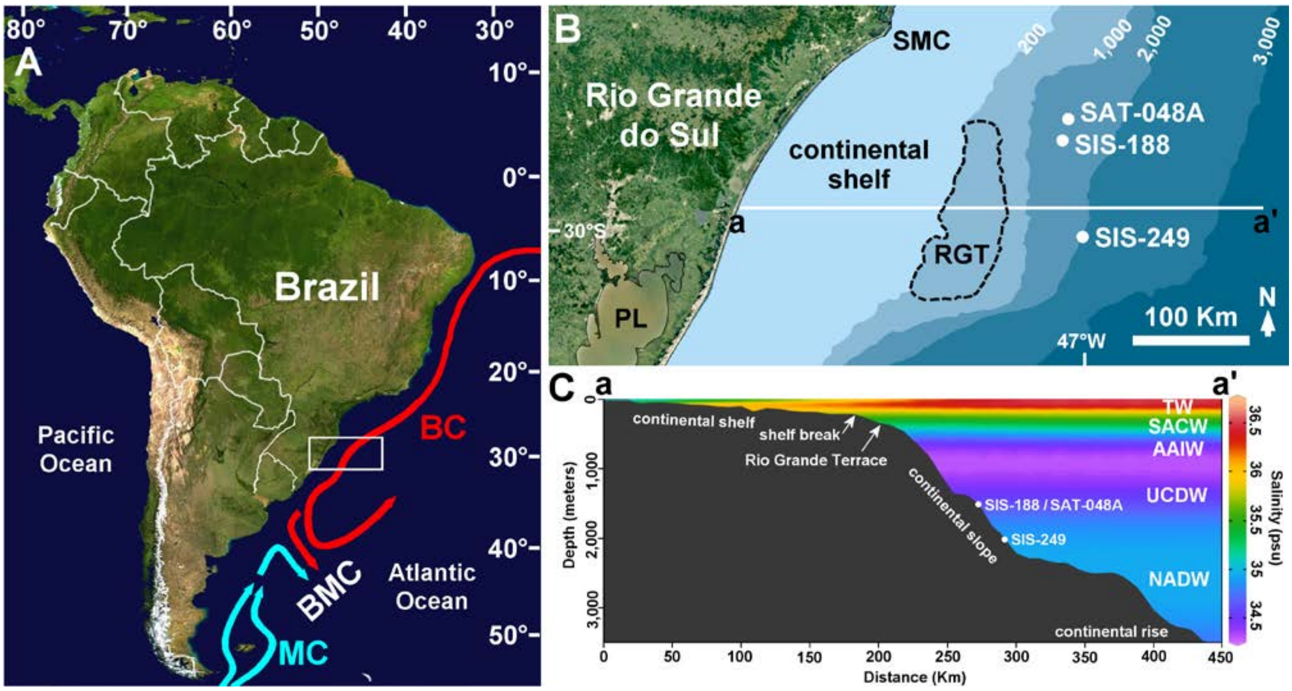

Figure 2. A - Blue Marble satellite image of South America showing the study area (white rectangle); BC: Brazil Current, MC: Malvinas Current, BMC: Brazil-Malvinas Confluence. B - The area highlighted in A showing the location of the studied cores (SMC: Santa Marta Cape, RGT: Rio Grande Terrace, PL: Patos Lagoon). C - Transect a-a' of the southern Brazilian continental margin indicated in B, showing the morphology, depth of the cores, and water masses in the cored area (TW: Tropical Water, SACW: South Atlantic Central Water, AAIW: Antarctic Intermediate Water, UCDW: Upper Circumpolar Deep Water, NADW: North Atlantic Deep Water) (modified from Lopes *et al.* 2021a).

Figura 2. A - Imagem de satélite Blue Marble da América do Sul mostrando a área de estudo (retângulo branco); BC: Corrente do Brasil, MC: Corrente das Malvinas, BMC: Confluência Brasil-Malvinas. B - Área destacada em A mostrando a localização dos testemunhos estudados (SMC: Cabo de Santa Marta, RGT: Terraço Rio Grande, PL: Lagoa dos Patos). C - Transecto a-a' da margem continental sul-brasileira indicado em B, mostrando a morfologia, a profundidade dos testemunhos e as massas de água na área do testemunho (TW: Água Tropical, SACW: Água Central do Atlântico Sul, AAIW: Água Antártica Intermediária, UCDW: Água Circumpolar Profunda Superior, NADW: Água Profunda do Atlântico Norte) (modificado de Lopes et al. 2021a).

2.2. Oceanographic setting

The cored depths are under the influence of the North Atlantic Deep Water (NADW) that flows southward between 2,000 and 4,000 m (Fig. 2C). The depths between 2,000 and ~1,000 m are occupied by the Circumpolar Deep Water (CDW), bisected by the NADW in upper and lower (UCDW and LCDW, respectively) water masses, whereas the Antarctic Intermediate Water (AAIW) occurs between 1,000 and 700 m, beneath the northward-flowing South Atlantic Central Water (SACW) and the surface Tropical Water (TW) carried by the southward-flowing Brazil Current (BC) (Reid, 1977; Stramma & England, 1977; Piola & Matano, 2009). The BC flows along the outer shelf-shelf break carrying the warm (>20°C) saline (>36 PSU) TW, which meets the cold (<15°C) and less saline (<34.2 PSU) subantarctic waters carried by the northward-flowing Malvinas Current

(MC), thus forming the Brazil-Malvinas Confluence (BMC) or subtropical convergence zone (Piola & Matano, 2009). The latitudinal position of the BMC shifts seasonally between about 39°S (summer) and 36°S (winter) due to stronger poleward influence of the BC or equatorward influence of the MC, respectively, and has also shifted in geological timescales related to glacial-interglacial cycles (Reid *et al.,* 1977; Matano *et al.,* 1993; Laprida *et al.,* 2011; Gu *et al.,* 2019).

The ocean circulation over the continental shelf off southern Brazil also varies seasonally. During spring-summer the cyclonic meanders of the BC and Ekmann transport driven by the strong prevailing NE winds carries the TW offshore, thus leading to upwelling of the nutrient-rich SACW along the bottom onto the outer-middle shelf up to the deep photic zone, whereas during autumn-winter the strong S-SW winds prevent upwelling (Emilsson, 1961; Pereira, 1989; Campos *et al.,* 2000; 2013; Brandini *et al.,* 2014). The inner-middle shelf is dominated by the TW during summer, whereas during winter there is stronger influence of the Sub-Antarctic Water (SAW), through the coastal branch of the MC (Ciotti *et al.,* 1995). The Brazilian Counter-Current (BCC) flows northward during winter along the inner-middle shelf carrying the coastal water (CW), a mixture of cold seawater from the BMC and freshwater discharge from the La Plata River and Patos Lagoon, with suspended sediment that constitutes the La Plata Plume (LPP), which increases phytoplankton productivity over the shelf (de Souza & Robinson, 2004; Campos *et al.,* 2013; Brandini *et al.,* 2014).

3. Materials and Methods

The piston cores SAT-048A, SIS-188, and SIS-249 were described by different authors as part of studies about the ocean paleoproductivity off southern Brazil (Petró, 2018; Rodrigues *et al.,* 2018; Frozza *et al.,* 2020; Lopes *et al.,* 2021a; Suárez-Ibarra *et al.,* 2022). The three cores encompass the late Pleistocene interval corresponding to the last glacial period (115.2-11.7 ka b2k), called Llanquihue glacial in South America (Heusser 1974), and part of the current Holocene interglacial (>11.7 ka b2k), thus encompassing the relatively warm interstadials MIS 5c, 5a and 3, and the cold stadials MIS 5d, 5b, 4 and 2, the latter including the last glacial maximum (LGM, 26.5-19 ka b2k). According to the age models derived from calibrated ^{14}C ages the sediments sampled by the core SIS-249 were accumulated between ~112 and 34 ka BP (Rodrigues *et al.,* 2018), whereas SAT-048A accumulated between 43 and 5 ka BP and SIS-188 between 47.7 and 7.2 ka BP (Frozza *et al.,* 2020; Gonçalves & Leonhardt, 2021; Petró *et al.,* 2021).

Although the age models show little overlapping between SIS-249 and SAT-048A/SIS-188, the combination of sedimentological data obtained in the three cores should provide a longer record spanning a substantial portion of the last glacial, and thus contribute to the understanding of long-term sedimentary dynamics on the lower slope off southern Brazil. As the optical microscope analyses showed that the sand-sized (>63 μm) carbonate sediments in the cores are of biogenic origin, i.e., mainly tests of benthic and planktonic foraminifera and some ostracods (Rodrigues *et al.,* 2018; Schmitt *et al.,* 2019; Lopes *et al.,* 2021a; Suárez-Ibarra *et al.,* 2022), the main objective of this study was to compare variations of carbonate sand in the cores and to evaluate whether such variations correlated with periods of increased deflation of continental dust, as proposed for the interval corresponding to the stadial MIS 4 recorded in the core SIS-249 (Lopes *et al.,* 2021a). It was hypothesized that higher eolian inputs of continental dust that reached the ocean during the last glacial, especially during the driest and coldest MIS 4 and 2, would have increased surface productivity, represented in the cores by higher proportions of biogenic carbonate sand.

The sedimentological analyses described here are based on samples obtained for micropaleontological studies with different sampling resolutions. For this analysis, the variations in the relative proportions of siliciclastic and carbonate sand found in the cores were compared by measuring the carbonate content obtained through dissolution with 10% hydrochloric acid (HCl) of sediment samples, whose grain sizes were measured using laser diffractometry before and after dissolution (Petró *et al.,* 2021; Lopes *et al.,* 2021a; Suárez-Ibarra *et al.,* 2022).

The variations of carbonate content along the three cores were then compared with paleoclimatic records to address the hypothesis that such variations could be correlated with episodes of increased dust deflation. The paleoclimatic records included the dated intervals of expansion of the Patagonian ice sheet glaciers in the central and southern Andes that increased the production of glaciogenic dust (Zech *et al.,* 2011; García *et al.,* 2018; Peltier *et al.,* 2021), and variations of the concentration of dust sourced from southern South American (SSA) and paleotemperatures measured in the EPICA Dome C (EDC) ice core from East Antarctica (Jouzel *et al.,* 2007; Lambert *et al.,* 2008; 2012). Although the records in the deep-sea cores and the EDC ice core may not exhibit direct temporal correspondence because of differences in distance from source areas, modes of dust transport (low vs. tropospheric circulation), and temporal resolution owing to differences in age models and sampling resolutions, the Antarctic record can be regarded as a proxy of episodes of dust deflation that may have reached the ocean surface off southern Brazil, considering the probable common dust source areas. As the deep-sea cores are of different lengths (Fig. 3) the sediment samples were calibrated according to the age models and aligned with the EDC3 time scale used in the Antarctic dust data (Parrenin *et al.,* 2007).

4. Results

The sediments sampled by the cores are mainly silt-dominated hemipelagic muds, with small proportions of clay and siliciclastic sand (Fig. 3). The three analyzed cores were sampled with distinct resolutions, which translated in differences in the number of measurements available for comparison. The coarser sampling resolutions in SIS-249 and SAT-048A did not record relatively short-term variations as observed in SIS-188, nevertheless, the cores exhibited comparable patterns of variation in the carbonate content, indicated by differences in the proportions of total and carbonate-free sand (Fig. 4A, B), and rates of sediment accumulation (Fig. 4C). The variations of the carbonate content exhibit general correspondence with the episodes of glacier advances in southern SSA, which are correlated with and higher dust concentrations (Fig. 4D) and coldest intervals in Antarctica (Fig. 4E).

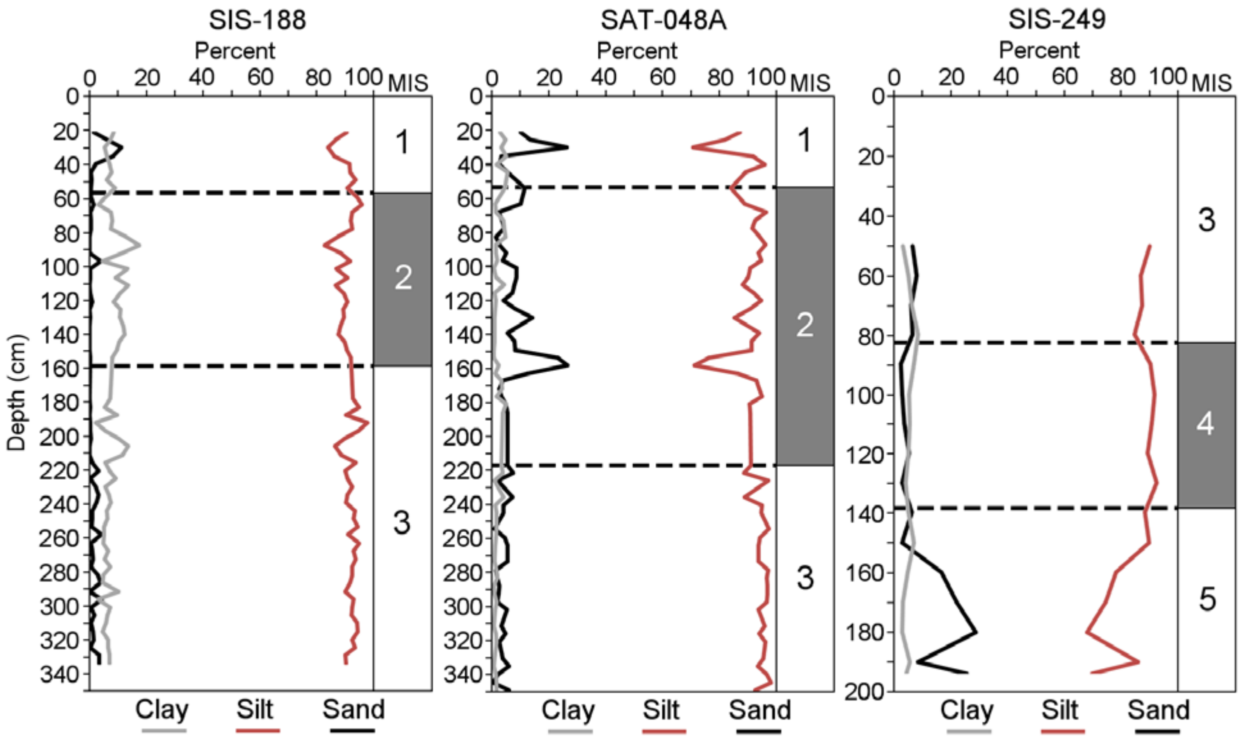

Figure 3 - Relative percentages of siliciclastic (carbonate-free) sediments in the studied cores.

Figura 3 - Porcentagens relativas de sedimentos siliciclásticos (não-carbonáticos) nos testemunhos analisados.

In all three cores, the proportions of clay and lithogenic silt exhibited small variation (Fig. 3). In the sand fraction, the proportion of carbonate in general was much higher than the siliciclastic content, and variations of the former are not matched by the latter in general. The exception is the core SIS-249, which exhibited the highest proportion of both siliciclastic and carbonate sand at its base, encompassing the MIS 5c to 5b interval (Fig. 4A, B). This high proportion of carbonate did not correspond to an interval of glacier expansion and significant dust input in the EDC ice core (Fig. 4D), therefore it does not seem to reflect increased productivity but could be related to sea-level oscillations (Lopes *et al.* 2021a). The lowest carbonate content in SIS-249 is recorded at the interval corresponding to MIS 5a, followed by a significant increase during the early-middle stadial MIS 4 and decreased during the later part of this stage. The higher proportion of carbonate during MIS 4 corresponds to an interval of Andean glacier advances and high dust concentrations and lower temperatures in Antarctica (Fig. 4D, E) of that stadial. The higher rates of sediment accumulation were also recorded during that stadial (Fig. 4C). The early part of the interstadial MIS 3 recorded in this core was characterized by a peak of carbonate sand, which may correspond to smaller peaks of dust accumulation in Antarctica (Fig. 4D), followed by lower content up to the core top.

The carbonate sand content in the lower part of the core SIS-188 (Fig. 4A), corresponding to the late MIS 3, exhibited high-amplitude and high-frequency variations, which were comparable to the general pattern recorded in SAT-048A despite the lower sampling resolution of the latter. The higher proportion of carbonate sand, although with significant variations, was recorded during the interval encompassing the early MIS 2 and LGM, which correlated with the highest dust concentration in the EDC ice core (Fig. 4D). A decrease of carbonate was observed after the LGM, followed by a small increase in the uppermost part of the core corresponding to the early MIS 1 and beginning of the postglacial marine transgression (PMT), despite the lowest dust concentration recorded in Antarctica at that time. The highest accumulation rates between the late MIS 3 and MIS 2 (Fig. 4C) correspond to glacial advances in Patagonia, increasing dust deposition in Antarctica (Fig. 4D), and the lowest temperatures of the last glacial (Fig. 4E).

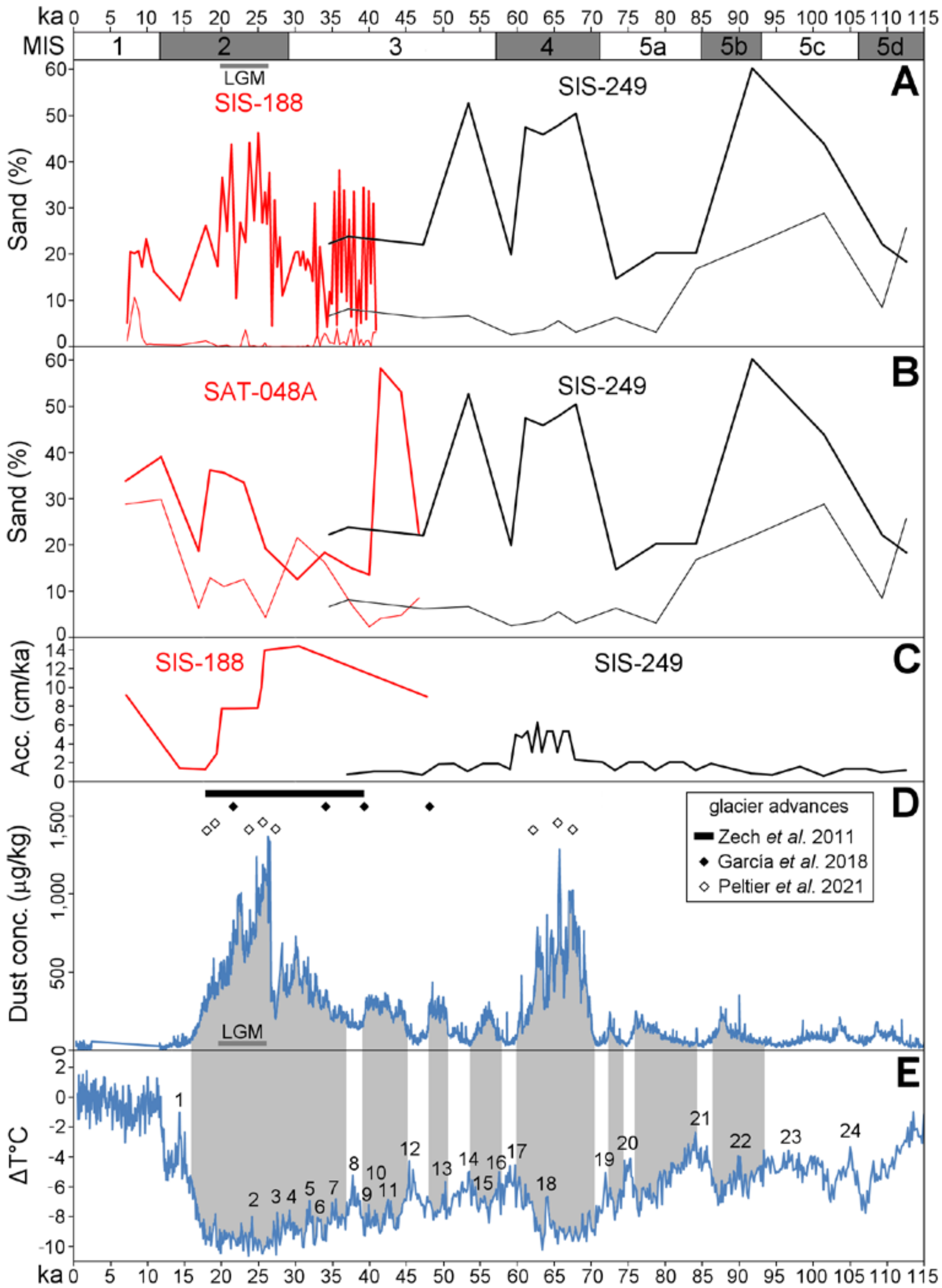

Figure 4. Relative proportions of carbonate (thick lines) and siliciclastic (thin lines) sand in the core SIS-249 compared to SAT-048 (A) and SIS-188 (B). C - Rates of sediment accumulation calculated for SIS-249 (Lopes *et al.*, 2021) and SIS-188 (Bottezini *et al.*, 2021). D - Dust concentrations in the EDC ice core (Lambert *et al.*, 2012) and intervals of expansion of Patagonian glaciers in the central (Zech *et al.* 2011) and southern Andes (García *et al.* 2018; Peltier *et al.* 2021). E - Temperature variations in Antarctica relative to the present from the EDC ice core (Jouzel *et al.*, 2007), the numbers indicate millennial-scale warming episodes, and the shaded areas point to the correspondence between colder intervals and dust accumulation.

Figura 4. Proporções relativas de areia carbonática (linhas grossas) e siliciclástica (linhas finas) no testemunho SIS-249 em comparação com os testemunhos SAT-048 (A) e SIS-188 (B). C - Taxas de acúmulo de sedimentos calculadas para SIS-249 (Lopes et al., 2021a) e SIS-188 (Bottezini et al., 2021). D - Concentrações de poeira no testemunho de gelo EDC (Lambert et al., 2012) e intervalos de expansão das geleiras patagônicas no centro (Zech et al., 2011) e sul (García et al., 2018; Peltier et al., 2021) dos Andes. E - Variações de temperatura na Antártica em relação ao presente no testemunho de gelo EDC (Jouzel et al., 2007), os números indicam episódios de aquecimento em escala milenial e as áreas sombreadas indicam a correspondência dos intervalos mais frios e a acumulação de poeira.

In the core SAT-048A (Fig. 4B) the highest proportion of carbonate sand was recorded at its lower part, representing the middle part of MIS 3, corresponding to a smaller pulse of dust concentration in Antarctica relative to MIS 4 and 2 (Fig. 4D). In the late MIS 3 the carbonate content was lower and even surpassed by an increase of siliciclastic sand close to the end of the stage. As in SIS-188, the carbonate content increased during the early part of the stadial MIS 2, reaching high values during the LGM that correspond to the interval of highest dust concentration and lowest temperatures in Antarctica (Fig. 4D, E). A decrease of carbonate sand in the later part of MIS 2 is followed by an increase at the transition to MIS 1 that reached a higher proportion than during the LGM, although it coincided with the interval of the lowest dust concentration in Antarctica. On the other hand, it also coincided with the onset of the sea level rise marking the PMT.

5. Discussion

The variations of the relative proportion of carbonate (biogenic) sand recorded in the cores SIS-188 and SAT-048A showed the highest and longest inputs at the intervals corresponding to the stadial MIS 2/LGM, and at some intervals of MIS 3. Together with the variation recorded during MIS 4 in SIS-249, the carbonate sand-rich levels seem to follow the temporal pattern of dust accumulation and lower temperatures in Antarctica (Fig. 4D, E). Because the variations of carbonate sand are not matched by variations in the siliciclastics (Fig. 3, Fig. 4A, B) the former can be interpreted as increases of biogenic inputs driven by changes of ocean paleoproductivity associated with higher deflation and deposition of dust on the ocean surface off southern Brazil. The higher rates of sediment accumulation in SIS-249 (MIS 4) and SIS-188 (late MIS 3-MIS 2) correlate with pulses of increased carbonate content but are not reflected in variations of lithogenic sediments (Fig. 3), thus indicating that accumulation rates were controlled mainly by inputs of biogenic sand. As the wind-blown dust that would have reached the ocean surface was mainly silt-sized, the absence of co-variation between lithogenic silt (Fig. 3) and carbonate sand indicates that most of the dust precipitated on the ocean surface did not reach the bottom, being probably used or adsorbed by organisms and/or dispersed in the water column by currents, despite remaining insoluble (or dissolving very slowly) after releasing dissolved nutrients in the upper ocean layer (Paparazzo *et al.,* 2018).

The lower rates of sediment accumulation during MIS 4 recorded in SIS-249 compared to late MIS 3-MIS 2/LGM as recorded in SIS-188 (Fig. 4C) could be explained by the shorter period of dust deflation and associated biological productivity during MIS 4.

The higher accumulation rates during MIS 3-MIS 2 are also reflected in the longest interval of dust deposition in Antarctica (Fig. 4D) and the shorter period (but larger extent) of glacier development in the southernmost part of South America (Peltier *et al.,* 2021). Nevertheless, the relative proportions of carbonate sand recorded during MIS 4 and MIS 2 were comparable, suggesting that dust-driven ocean productivity was not directly related to the volumes of dust deflated from the source areas or the length of the interval of deposition. Although several small pulses of dust accumulation are recorded in the EDC ice core, correlated with colder episodes from MIS 5 to MIS 3 (Fig 4D, E), the apparent lack of correspondence in SIS-249 (Fig. 4A, B) could indicate negligible influence of these inputs on the ocean productivity along the SW Atlantic, although it may also result from the coarser sampling resolution in SIS-249.

The changes in the relative proportion of carbonate sand along the cores indicated variations in the relative abundance of benthic foraminifera that grew *in situ* at the bottom, as well as planktonic species whose empty tests sank to deeper areas (Rodrigues *et al.,* 2018; Petró *et al.,* 2021). In fact, the sand fraction on the slope along southeastern-southern Brazil is dominated by tests of planktonic foraminifers (Kowsmann *et al.,* 1977), which can be attributed to high ocean paleoproductivity during the last glacial period. The nutrients contained in the dust deposited on the ocean surface fuel phytoplankton blooms (mainly diatoms and coccolithophores), which in turn are used by foraminifers and other organisms that opportunistically proliferate in the upper water column. The empty foraminifer tests and phytodetritus in aggregates or contained in fecal pellets sink to the sea bottom. For instance, the relationship between (paleo)productivity in the upper water column and benthic foraminifers has been explained in terms of the ecological strategies of foraminifera taxa. Higher relative abundances of epifaunal benthic foraminifera *Epistominella exigua* and *Alabaminella weddellensis* found at intervals corresponding to MIS 4-MIS 3 in SIS-249 could have resulted from opportunistic proliferation in response to higher inputs of phytodetritus produced by increased surface productivity, possibly on seasonal scales (Thomas *et al.,* 1995; Thomas & Gooday, 1996; Sun *et al.,* 2006; Rodrigues *et al.,* 2018). A similar mechanism operating under glacial conditions during the middle-late Pleistocene was inferred in the Santos Basin to the north (25°S) from a core obtained at a water depth of 2,220 m (de Almeida *et al.,* 2015).

The increases in sand-sized biogenic carbonate recorded in the deep ocean probably reflect the higher proliferation of diatoms and other photosynthesizing organisms on the ocean surface in response to increased nutrient availability provided by wind-blown dust. The fluctuations of carbonate sand content in the sampled cores exhibited a general pattern that could be related to similar environmental conditions during the stadials MIS 4 and 2 and interstadial MIS 3 (see item 5.1. below), although some peaks of carbonate input could have other causal mechanisms. In the core SIS-249, the high proportion of both siliciclastic and carbonate sand at its base could have resulted from increased downslope mass movements caused by instabilities generated on the upper slope/RGT related to sea-level oscillations during the late MIS 5 (Lopes *et al.,* 2021a). The highest sea levels (+6 to + 9 m above the present) of that stage occurred during the last interglacial (LIG, substage 5e), and were followed by positive oscillations of smaller amplitude during the interstadials 5c and 5a (Fig. 4D; Potter *et al.,* 2004; Hearty *et al.,* 2007; Dutton & Lambeck, 2012). Geological and fossil records along the coast of Rio Grande do Sul indicate a higher sea level (up to +4 m above the present) around 104 ka b2k (MIS 5c) followed by the MIS 5b sea level fall, which in theory could have triggered mass movements on the outer slope (Lopes *et al.,* 2020a).

In a similar way, the decrease of carbonate sand and increase of silicilastic sand recorded at the interval corresponding to the latest MIS 3 in core SAT-048A (Fig. 4B), could be related in part by sand transfer from the RGT to the lower slope as a result of the sea-level fall following a positive eustatic oscillation recorded in southern Brazil (Dillenburg *et al.,* 2019). Sea level rose from about -80 m relative to the present during MIS 4 (Grant *et al.,* 2012) and reached about -23 to -5 m between 47.7 and 36.2 ka BP, consistent with an estimated mean global sea level of -38 m between 57 and 30 ka BP (Pico *et al.,* 2016). The opposite pattern recorded in SIS-188, however, characterized by relatively similar carbonate but much lower siliciclastic sand content compared to SAT-048A during the latest MIS 3 (Fig. 4A) suggests other influences, such as changes in oceanographic conditions. The carbon isotope ratios ($\delta^{13}C$) in foraminifers obtained in the cores are less positive during the intervals of ~55-50 ka BP and ~45-40 ka BP (Rodrigues *et al.,* 2018, Frozza *et al.,* 2020; Petró *et al.,* 2021), roughly corresponding with peaks of carbonate input recorded in SIS-249 and SAT-048A, respectively (Fig. 4B). This correspondence between less positive $\delta^{13}C$ and peaks of carbonate deposition could have resulted from stronger influence of ^{13}C-depleted and nutrient-rich Antarctic-sourced waters (Lopes *et al.,* 2021a),

5.1. Environmental conditions in SSA during the last glacial period

The apparent correlation between the increases of biogenic carbonate sand recorded on the three cores and the colder intervals with the highest dust concentration in Antarctica (Fig. 4D, E) during the last glacial suggest that climate-driven inputs of eolian-sourced glaciogenic dust could have contributed to increased ocean productivity off southern Brazil. This hypothesis can be understood in terms of the mechanisms of generation and transport of the dust that reached Antarctica and southern Brazil, controlled by the environmental conditions recorded in SSA during the last glacial period.

The higher dust concentrations in Antarctica correspond to the stadials MIS 4 and 2, the driest and coldest intervals of the last glacial period. Although isotopic records in deep sea and ice cores showed that the Northern Hemisphere ice sheets were ~25% larger during MIS 2 compared to MIS 4 (Clapperton, 1993), paleoceanographic data from the southeastern Pacific and South Atlantic indicate similar, full glacial conditions characterized by colder temperatures during both stadials (Heusser *et al.,* 2006; Kaiser *et al.,* 2005; Kaiser & Lamy, 2010; Barker & Diz, 2014). On land, glaciogenic deposits showed maximum ice extent in the southern Andes around 67.1 ka b2k, coeval with the advance of mountain glaciers in New Zealand around 65.1 ka b2k, indicating a worldwide cooling during MIS 4 comparable to MIS 2 (Schaefer *et al.,* 2015; Doughty *et al.,* 2021; Peltier *et al.,* 2021). The largest extent of the Andean glaciers during MIS 4 was attributed to the higher moisture compared to MIS 2, although the latter was characterized by a longer period of glacier growth (Peltier *et al.,* 2021).

Although MIS 4 records are scarce compared to later intervals, the available evidence shows that in SSA this stadial was characterized by northeastwards expansion of dry environments, and increased eolian transport by strong SW winds generated by the South Pacific Anticyclone (SPA) of glaciogenic fine sediments that accumulated on the sand sea and the surrounding loess belt that forms the Pampean eolian system of Argentina (Iriondo, 1999; Zárate & Tripaldi, 2012). The conditions during MIS 2 were similar, but better represented by different records that indicate dry climate, increased eolian deflation, reduced vegetation cover, and replacement of humid grassland steppes by xerophytic shrubby communities across the Pampas from northeastern Argentina to southern Brazil (Quattrochio & Borromei, 1998; Behling *et al.,* 2005; Tonello and Prieto, 2010; Mourelle *et al.,* 2020).

The interstadial MIS 3 in SSA was warmer and wetter compared to the stadials MIS 4 and 2, with more developed vegetation cover and soils (Gasparini *et al.,* 2016).

Nevertheless, dated moraine deposits in the southern Andes indicate that glaciers of the Patagonian ice sheet not only expanded but reached larger sizes compared to MIS 2 (García *et al.,* 2018). The increases in dust concentration in Antarctica during the late MIS 3 (<40 ka b2k, Fig. 4D) correspond to stronger eolian deflation coeval with the expansion of glaciers that started around 39 ka b2k in the central Andes (Zech *et al.,* 2011) and around 48 ka b2k in the southern Andes (García *et al.,* 2018). These episodes of glacier expansions would have been driven by the equatorward shift of the westerly winds, as recorded during MIS 4 and MIS 2 (see section 5.2. below).

Besides intervals of high dust accumulation related to strong stadial conditions, the EDC ice core exhibits several smaller dust peaks correlated with lower temperatures. intercalated with several millennial-scale warming episodes, called Antarctic isotopic maxima (AIMs), during which dust inputs were reduced (Fig. 4D, E), This pattern suggests that dust deflation was a prevalent feature of the last glacial, reduced or interrupted by anomalous warmer episodes. Although the exact causal mechanisms are unknown, it is possible that changes in atmospheric circulation, increased rainfall, and soil stabilization during the relatively warmer AIMs could have reduced dust deflation in SSA.

The geological records in central Argentina point to an alternation between subhumid and humid phases related to climate oscillations in centennial to millennial scales during MIS 3 (Clapperton, 1993; Voelker, 2002; Zárate *et al.,* 2016). Although wetter conditions probably decreased eolian deflation, ocean fertilization could have been fueled by short-term, episodic dust storms during subhumid phases (Paparazzo *et al.* 2018), consistent with small peaks of increased dust accumulation in Antarctica centered at ~59, ~50, and ~43 ka b2k (Fig. 4D) chronocorrelated with peaks of biogenic carbonate recorded in the three cores (Fig. 4A, B). It is noteworthy that the peaks of carbonate sand at ~44 and ~41 ka b2k recorded in SAT-048A (Fig. 4B) and probably SIS-188 (Fig. 4A) do not only match the dust record in Antarctica (Fig. 4D) but also the higher dust accumulation at ~43 and ~41 ka b2k in the Argentinean Pampas related to increased inputs from the PAP, which would have been drier than the Pampas at that time (Torre *et al.* 2019). Modeling and observational data showed that dust from the PAP can reach the South Atlantic off Rio Grande do Sul today (Gaiero *et al.,* 2013), and that dust may have thus contributed to a higher surface productivity. Consequently, primary productivity leading to inputs of phytodetritus should have allowed benthic foraminifers *E*. *exigua* and *A*. *weddellensis* to proliferate during MIS 3 as recorded in SIS-249 (Rodrigues *et al.,* 2018).

5.2. Mechanisms of dust generation and transport during the last glacial

The increased deflation, transport, and accumulation of dust during glacial periods compared to interglacials were favored by three major factors: a) enlarged dust source areas due to reduced vegetation cover and less soil moisture, b) increased eolian processes due to stronger winds, and c) reduced hydrological cycle that allowed the dust to remain in suspension for longer periods (Mahowald *et al.,* 1999). Although the intervals of highest peaks of dust accumulation in Antarctica correspond to the coldest stadials recorded in the EDC ice core, the smaller peaks correlated with smaller-amplitude cooling episodes (Fig. 4D, E) indicate a close climatic control on the deflation of dust from SSA.

The entrainment and transport of glacially generated dust in SSA seem to have been favored by a combination of changes in ocean and atmospheric circulation (Kaiser *et al.,* 2005; Kaiser & Lamy, 2010; Peltier *et al.,* 2021). The temperatures ~5° to 7°C lower than today caused the expansion of marginal marine ice around Antarctica, leading to the equatorward shift of the Antarctic circumpolar current (ACC), southern polar (SPF), and subantarctic (SAF) fronts, and the southern westerly winds (SWW) belt, or westerlies. The SWW is a belt of quasi-permanent cyclonic waves extending today between ~40° and ~70°S, but different proxies indicate that it shifted equatorward by 5°-6° to the north during MIS 4 and 4°-5° during the LGM, and its northern limit reached up to ~28°S (Heusser, 1989; Lamy *et al.,* 1998; Iriondo, 2000; Mohtadi & Hebbeln, 2004; Kaiser *et al.,* 2005). The shifted fronts also strengthened the polar incursions that reached South America (Ledru *et al.,* 1996; 2001).

As the westerlies reach the east side of the Andes they are forced upwards, discharging high amounts of precipitation (>2,000 mm annually in southern Chile) that feeds the southern and northern Patagonian ice sheets, which were expanded further to the north during stadials (Fig. 5A) as a result of the equatorward shift of the SWW (Kaiser & Lamy, 2010). There is a positive correlation between periods of larger glacier extent and dust deflation during the last glacial in SSA, represented by the highest concentrations of dust in Antarctica (Fig. 4D). The advances of mountain glaciers in the central-southern Andes produced high amounts of fine rock flour through increased glacial weathering (Basile *et al.,* 1997). That material was redistributed by meltwater rivers flowing toward the Atlantic and deposited on glacial outwashes developed on the large areas of the Argentinean continental shelf subaerially exposed because of the lower relative sea levels during the last glacial (Sugden *et al.,* 2009; Kaiser & Lamy, 2010). The higher dust fluxes in Antarctica during MIS 2 compared to MIS 4 (Fig. 4D) could be explained by the lower sea levels (~-120 m) reached during the former (Rohling *et al.,* 1998; Rabineau *et al.,* 2006), compared to ~-80 m during the latter (Grant *et al.* 2012), thus exposing larger areas of the continental shelf off Patagonia covered by glacial outwash, which enlarged the dust source area (Iriondo, 2000).

The expanded glaciers also contributed to increased eolian activity through katabatic winds produced by gravity and thermal gradients (Bullard, 2013). The westerlies are cooled and accelerated as they cross the highest Andes, descending on the lee side of the mountains as dry and relatively warm, strong foehn winds (locally called *zonda*) that generate the orographic desert stretching from central-western Argentina to Patagonia (Kaiser & Lamy, 2010; Gili *et al.,* 2017). The combination of the SWW shifted up to ~28°S, stronger westerly *zonda* winds, and lower Earth obliquity, with minima centered at ~70 ka b2k and ~29 ka b2k, would have decreased seasonality and caused high latitude environments to expand toward lower latitudes (van den Heuvel, 1966; Williams, 1993), leading to a ~1,500 km northeastward expansion of the Arid Diagonal dry environments up to the Argentinean Pampas, Uruguay and southern Brazil (Bruniard, 1982; Prieto, 1996; Iriondo, 1999; Lopes *et al.,* 2023).

The expanded arid environments, reduced plant cover, and stronger winds resulted in the deflation of the glaciogenic silt-dominated dust accumulated on the Andean piedmont, which included not only newly generated particles but also silt deflated from older loess deposits on the Argentinean plains (Iriondo, 1999). Geomorphic records in the Pampean region of Argentina indicate prevailing S-SW winds generated by the South Pacific anticyclone and stronger polar incursions, which in conjunction with the *zonda* winds deflated and carried dust from the CWA and northern Patagonia across the Pampas plains, whereas dust from the PAP was carried southeastwards by the LLJ (Iriondo, 1999; Gaiero *et al.*, 2007; Zárate & Tripaldi, 2012; Gili *et al.,* 2017; Torre *et al.,* 2022).

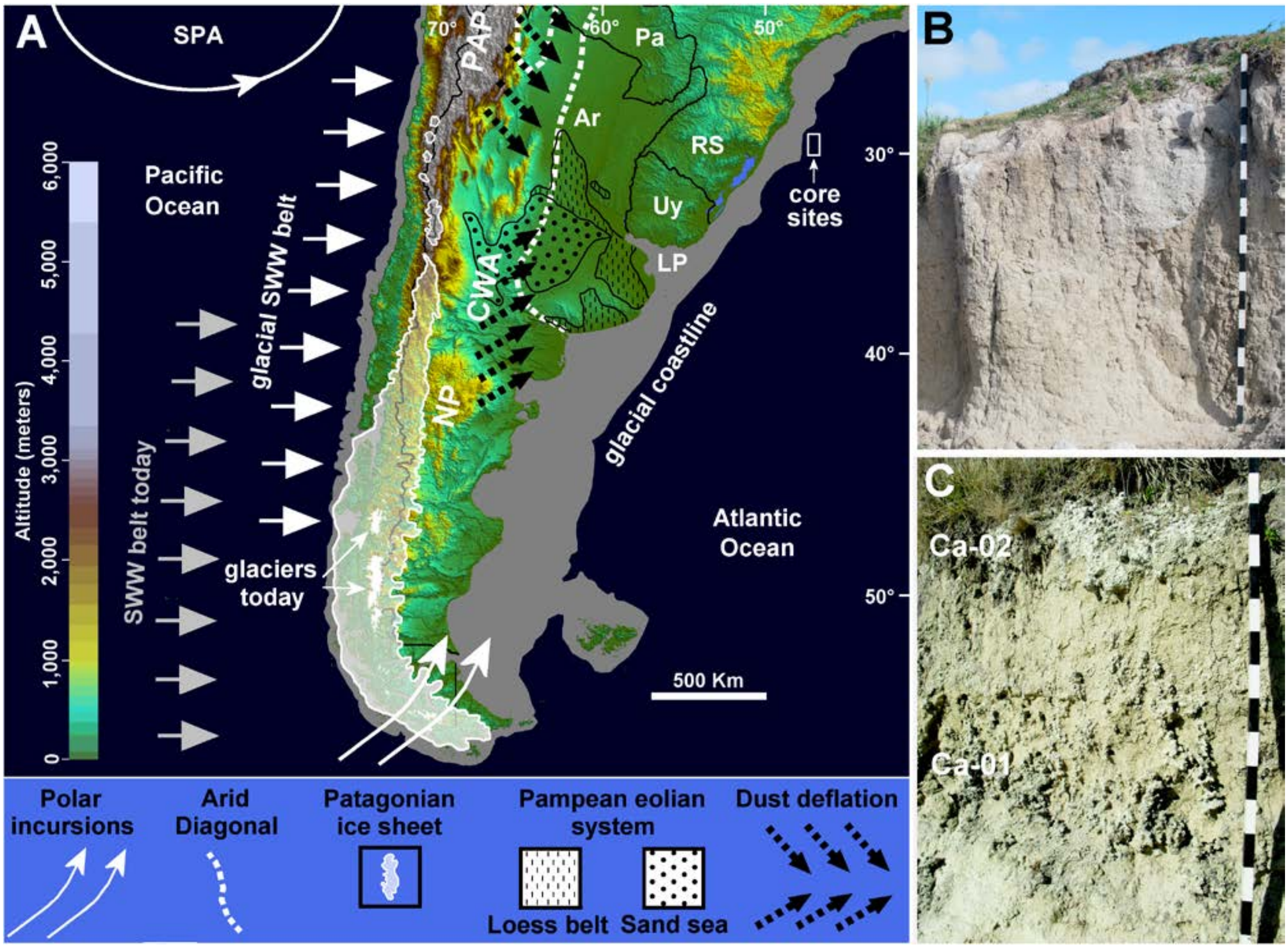

Figure 5. A - Digital elevation image showing th physical configuration of southern South America during the stadial MIS 2, indicating the dust sources (PAP: Puna-Altiplano Plateau, CWA: Central-Western Argentina, NP: Northern Patagonia); the glacial and current extent of the Andean glaciers (after Clapperton 1993) and SWW belt are shown for comparison (SPA: South Pacific Anticyclone, Ar: Argentina, Pa: Paraguay, RS: Rio Grande do Sul, Uy: Uruguay, LP: La Plata River). B - Loess deposits (Cordão Formation) in the southern coastal plain of Rio Grande do Sul (each division of the scale = 10 cm). C - Pedogenic carbonate horizons presumably formed during MIS 4 (Ca-01) and MIS 3-MIS 2 (Ca-02).

Figura 5. A - Imagem de elevação digital mostrando a configuração física do sul da América do Sul durante o estadial MIS 2, indicando as fontes de poeira (PAP: Planalto Puna-Altiplano, CWA: Centro-Oeste da Argentina, NP: Norte da Patagônia); a extensão glacial e atual das geleiras andinas (segundo Clapperton 1993) e o cinturão dos SWW são mostrados para comparação (SPA: Anticiclone do Pacífico Sul, Ar: Argentina, Pa: Paraguai, RS: Rio Grande do Sul, Uy: Uruguai, LP: Rio da Prata). B - Depósitos de loess (Formação Cordão) na planície costeira sul do Rio Grande do Sul (cada divisão da escala = 10 cm). C - Horizontes de carbonatos pedogênicos presumivelmente formados durante MIS 4 (Ca-01) e MIS 3-MIS 2 (Ca-02).

Based on the physical properties and mineralogical composition, the Pampean loess is likely the main source of loess deposits in the southern coastal plain of Rio Grande do Sul state (CPRS), in southernmost Brazil (Lopes *et al.,* 2016a), although contributions from the PAP cannot be discarded, as described above. The loess in the CPRS is represented by a calcrete-bearing loess mantle (Cordão Formation, Fig. 5B) accumulated between the late MIS 3 and MS 2 (Lopes *et al.,* 2016a). Calcrete-bearing silty sand with luminescence ages of ~71-73 ka b2k (Fig. 5C, Lopes *et al.,* 2016b) found in the underlying Santa Vitória Alloformation (Lopes *et al.*, 2021b) point to eolian dust deposition also during MIS 4. The wind-blown dust probably accumulated on the adjacent >50 km-wide portion of the continental shelf off Rio Grande do Sul that was subaerially exposed during the last glacial and reached the Atlantic Ocean. The possibility of eolian-sourced dust from SSA reaching the cored area is indicated by the presence in SIS-188 of pollen of *Araucaria* (Bottezini *et al.,* 2022) probably carried from the Araucárias Plateau in the northern Rio Grande do Sul (Fig. 6A), besides pollen of *Nothofagus* (southern beech) characteristic of forests of southern Patagonia found in a core obtained in the upper slope some 240 km to the NE of SIS-188 (Gu *et al.,* 2017). These scenarios are consistent with transport by increased W-SW winds related to the equatorward shift of the SWW belt (Fig. 5A).

Loess deposits have been identified so far on the southern coast of Rio Grande do Sul, therefore its total extent to the north is yet unknown. Nevertheless, eolian dust can be carried in suspension for >1,000 km (Maher *et al.,* 2010), therefore dust deflated from Argentina could have been transported by strong S-SW winds up to the ocean area off the northern coast of Rio Grande do Sul sampled by the cores, which could have received dust deflated from the PAP as well (Gaiero *et al.,* 2013). As shown in Figure 1, dust deflated from CWA today can stretch for hundreds of kilometers over the ocean, and if this process was more frequent and intense during the last glacial due to stronger winds as suggested by different proxies, the sediments deposited on the ocean surface could have supplied significant amounts of nutrients that would have fueled higher surface productivity. The higher water vapor and rainfall over the ocean compared to dry continental areas would have favored precipitation of dust (wet removal) which can be twice as large than removal under dry conditions (Cosentino *et al.,* 2019).

As a result of the warmer and wetter climate during the Holocene, the marginal ice around Antarctica was reduced, leading to a poleward migration of the SAF, SPF and SWW, and to a retreatment of the glaciers of the central Andes, which today are restricted to southernmost Patagonia (Fig. 5A). The arid environments retreated to the area occupied today by the modern Arid Diagonal; the Pampas were occupied by subtropical vegetation, and soil development stabilized the landscape (Prieto, 1996; Iriondo, 1999), which together with decreased eolian activity, reduced dust deflation. Although dust storms occur today and provide nutrients to the South Atlantic, the amount of dust accumulated in the Argentinena Pampas is smaller compared to the accumulation during glacial times (Cosentino *et al.,* 2019; Gassó & Torres, 2019).

5.3. Other drivers of paleoproductivity off southern Brazil: a critical review

The hypothesis of ocean fertilization by wind-blown glaciogenic dust deposited off southern Brazil presented here involves mechanisms that are well known from different records, as described above, although it may not have been the only driver of ocean paleoproductivity. Different studies have discussed variations of ocean paleoproductivity in southern Brazil from other proxies such as microfossils and stable isotopes, attributing nutrient inputs to offshore areas sampled by the cores to essentially three mechanisms: a) terrigenous sediments carried through paleochannels cutting across the shelf during glacial lowstands, b) sediments carried in suspension by the La Plata River plume (LPP), and c) upwelling of nutrient-rich waters. A close examination of these mechanisms, however, revealed some problems that hinder the establishment of causal relationships with the recorded changes in productivity.

5.3.1. Paleochannels

Some studies correlated higher productivity recorded in deep sea cores to inputs of nutrient-rich terrigenous sediments supplied via fluvial systems crossing the subaerially exposed continental shelf of the northern coast of Rio Grande do Sul, which presumably discharged close to the shelf break (and thus close to the cored areas described here) during glacial lowstands (Bottezini *et al.,* 2022; Suárez-Ibarra *et al.,* 2022). This interpretation, however, posits two main problems. First, the continental shelf off Rio Grande do Sul is mostly devoid of drowned fluvial systems, or paleochannels, as revealed by the mapping surveys in the 1970s (Kowsmann *et al.,* 1977; Zembruscki, 1979). This probably results from the development of middle-late Pleistocene barrier-lagoon systems that compose most of the coastal plain of Rio Grande do Sul (CPRS) that caused the fluvial discharges that once reached the shoreline to become trapped on the coastal lagoons (Villwock & Tomazelli, 1995). The only fluvial drainages that seem to have been active during the last glacial are found off the southern coast of Rio Grande do Sul, represented by the La Plata River paleochannel (Kowsmann *et al.,* 1977; Corrêa *et al.,* 2014; Lantzsch *et al.,* 2014) and those associated with permanent inlets crossing the Pleistocene barriers, near the outlet of Patos Lagoon (Abreu & Calliari, 2005) and on the now-closed outlet of Mirim Lagoon some 60 km to the south (Barboza *et al.,* 2021b), both located >400 km south of the cored area.

Second, few fluvial systems discharge on the shoreline in the northern CPRS today (Fig. 6A), and it seems unlikely that these reached close enough of the shelf break to influence productivity in areas close to the cored sites, even when sea levels were much lower than today. Seismic and acoustic surveys showed that the surface of the RGT does not exhibit fluvial paleochannels of continental origin cutting across its surface, although it exhibits erosive terraces and gullies generated by currents and downslope mass movements (Butler, 1970; Lisniowki & Alves, 2018a,b; Alves *et al.,* 2021; Lopes *et al.,* 2021a). Considering the low gradient (0.027°–0.125°) and large width (~170-180 km) of the continental shelf (Dillenburg & Barboza, 2014), and the lowest sea levels of ~-80 m during MIS 4 and ~-120 m during MIS 2 (Rabineau *et al.,* 2006; Grant *et al.,* 2012), the paleo-shorelines would have been located >60 km and >100 km east relative to the modern shoreline, respectively (Fig. 6A), thus implying that the cored sites would have been located >100 km far from the paleoshorelines (Fig. 6B). Moreover, due to the prevailing SW-NE longshore transport (littoral drift) (Lima *et al.,* 2001), it is likely that suspended fine sediments and organic matter discharged by fluvial systems reaching the paleoshorelines would have been dispersed by coastal dynamics before reaching the shelf break and beyond.

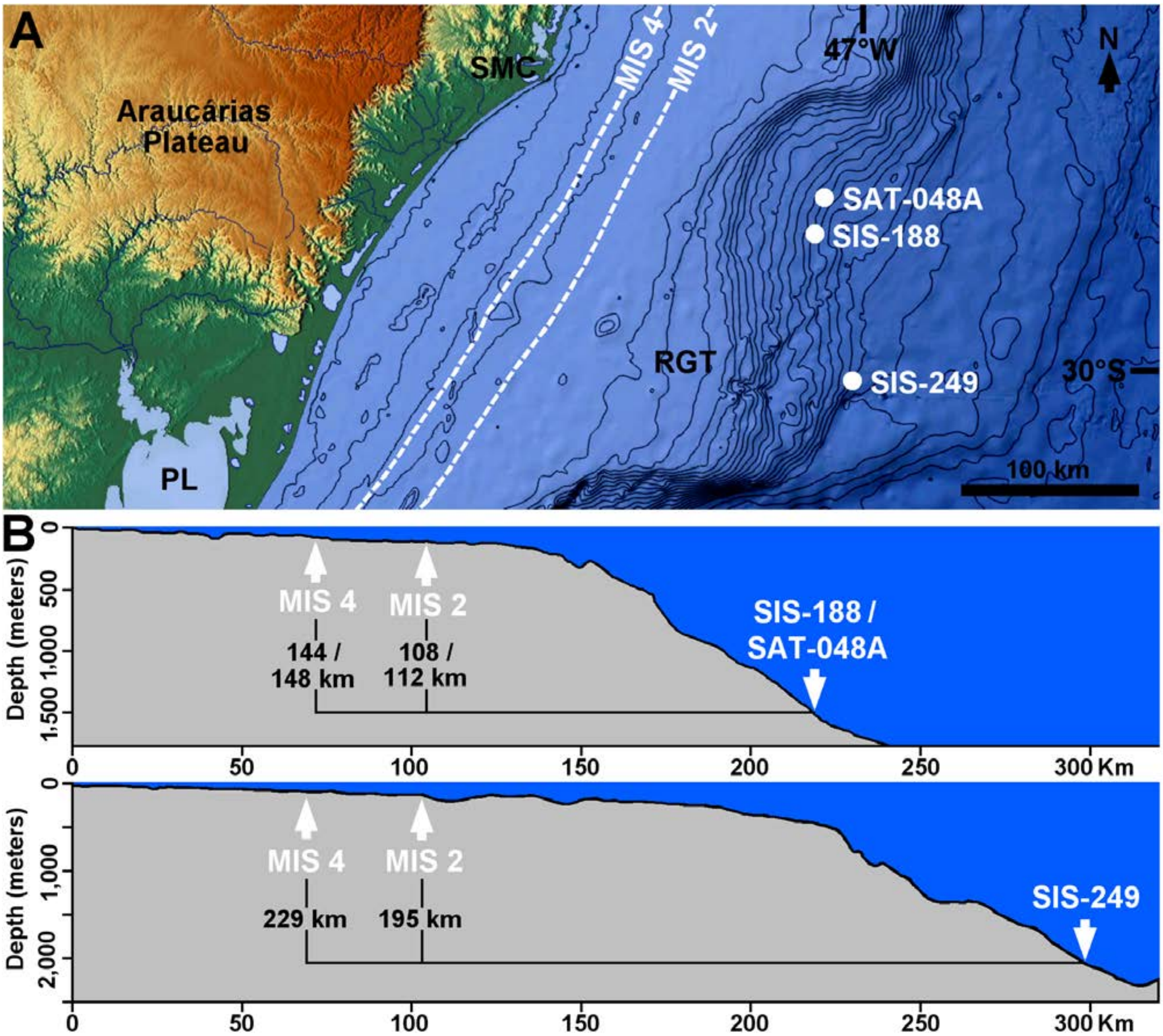

Figure 6. A - Digital elevation map of the northern coast of Rio Grande do Sul showing the location of the cores and the approximate positions (white dashed line) of the MIS 4 (-80m) and MIS 2 (-120m) paleoshorelines (PL: Patos Lagoon, RGT: Rio Grande Terrace, SMC: Santa Marta Cape); bathymetric lines georeferenced relative to the SIRGASS 2000 datum provided by the Serviço Geológico do Brasil (https://www.cprm.gov.br/publique/Geologia/Geologia-Marinha/Projeto-Batimetria-3224.html). B - Transects from the modern coastline to the cored sites, showing their distances relative to the MIS 4 and MIS 2 paleoshorelines.

Figura 6. A - Mapa de elevação digital do litoral norte do Rio Grande do Sul mostrando a localização dos núcleos e as posições aproximadas (linha tracejada branca) das paleo-linhas de costa durante o MIS 4 (-80m) e MIS 2 (-120m) (PL: Lagoa dos Patos, RGT: Terraço do Rio Grande, SMC: Cabo de Santa Marta); linhas batimétricas georreferenciadas relativas ao Datum SIRGASS 2000 fornecidas pelo Serviço Geológico do Brasil (https://www.cprm.gov.br/publique/Geologia/Geologia-Marinha/Projeto-Batimetria-3224.html). B - Transectos desde a costa moderna até os locais testemunhados, mostrando suas distâncias em relação às paleo-linhas de costa do MIS 4 e MIS 2.

5.3.2. The La Plata Plume

Another proposed source of nutrients that increased paleoproductivity off southern Brazil has been the La Plata River plume (LPP) or Plata River plume (PRP) (Gu *et al.,* 2017; Portilho-Ramos *et al.,* 2019). The freshwater discharges from the fluvial systems of the Paraná and Uruguay river basins converge on the La Plata estuary (Fig. 5A), and upon reaching the Atlantic Ocean are carried northward along the coasts of Uruguay and Rio Grande do Sul, mixing together with shelf water of subantarctic origin (SAW) and freshwater outflow of the Patos Lagoon to form the coastal water (CW). The LPP is a cold (Fig. 7A), low salinity tongue that occupies the uppermost 5-20 m of the water column, being transported northeastwards by the Brazilian Coastal Current (BCC) that flows parallel to the coast carrying suspended fine sediments and nutrients that increase phytoplankton productivity over the inner-middle shelf as indicated by high chlorophyll-a concentrations (Fig. 7B) (Ciotti *et al.,* 1995; Campos *et al.,* 1999; Piola *et al.,* 2000; de Souza & Robinson, 2004; Alves *et al.,* 2021). The LPP is separated from the BC by a dynamic shear zone along the middle shelf characterized by vortices and meanders (Fig. 7A, B).

The dynamics of the LPP are controlled mainly by seasonal changes in wind regimes, and secondarily by the volume of continental discharges from the La Plata River and Patos Lagoon. During winter, the strong S-SW winds associated with cold fronts generated by polar advection cause onshore contraction of the LPP, which is transported northeastwards along the inner shelf, reaching as far as ~23°S under favorable conditions. During summer the prevailing NE winds restrict the LPP to areas closer to the La Plata estuary and cause Ekman drift that results in the separation of the plume from the coast, reaching up to the shelf break in front of the estuary (Pimenta *et al.,* 2005; Piola *et al.,* 2005; Gonzalez-Silvera *et al.,* 2006; Matano *et al.,* 2014; Berden *et al.,* 2020).

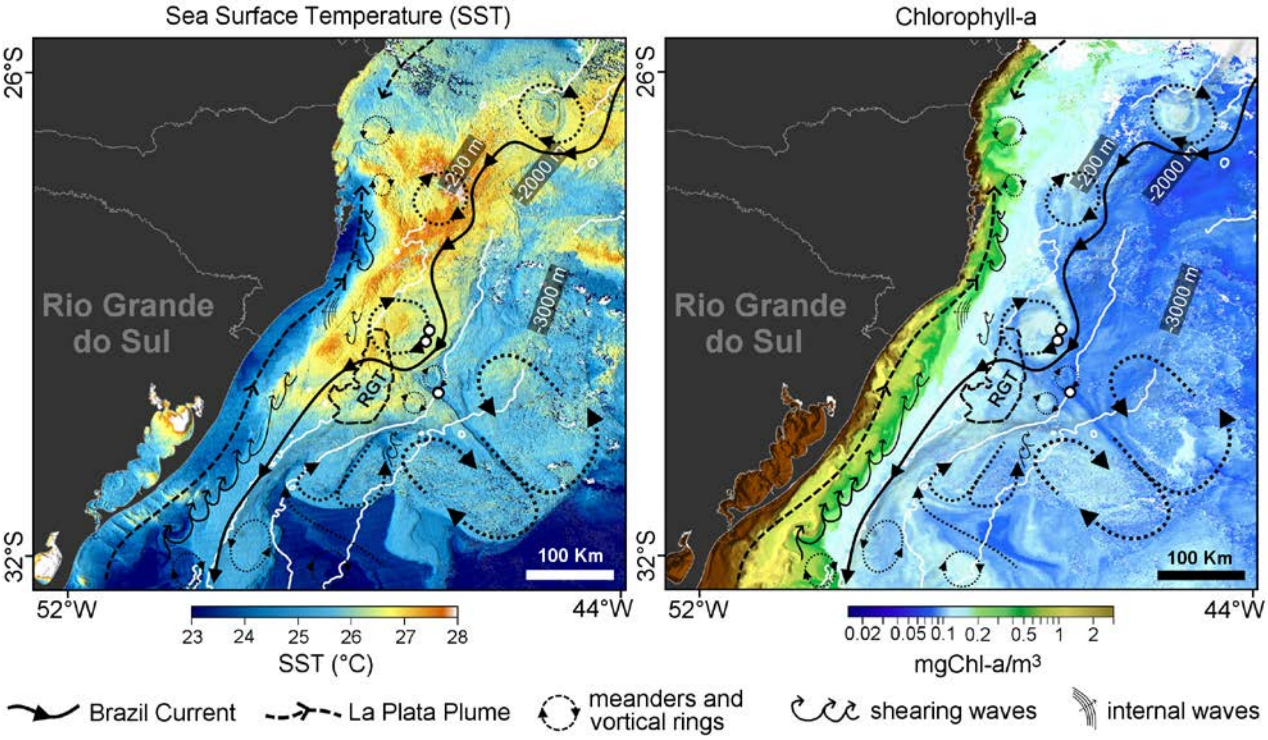

Figure 7. Composition of images obtained by Aqua, Terra, and Suomi NPP satellites between 27th and 29th February 2020 showing summer temperatures (A) and chlorophyll-a concentrations (B) on the ocean surface along the southern Brazilian continental margin (Modified from Alves *et al.* 2021). The cold, eutrophic La Plata Plume water is clearly distinguished from the warm, oligotrophic Brazil Current. The white circles show the location of the cores described in the text (RGT: Rio Grande Terrace).

Figura 7. Composição das imagens obtidas pelos satélites Aqua, Terra e Suomi NPP entre 27 e 29 de fevereiro de 2020 mostrando temperaturas (A) e concentrações de clorofila-a (B) na superfície do oceano durante o verão ao longo da margem continental sul brasileira (Modificado de Alves et al. 2021). A água fria e eutrófica da Pluma do Rio da Plata distingue-se claramente da Corrente do Brasil quente e oligotrófica. Os círculos brancos mostram a localização dos testemunhos descritos no texto (RGT: Terraço do Rio Grande).

The main problem with the proposed LPP as a source of nutrients to offshore areas north of the La Plata estuary is that no mechanism was provided so far to explain the required cross-shelf transport of the plume from the inner-middle shelf. Although the exchange occurs off the La Plata estuary under oceanographic conditions related to the BMC (Pimenta *et al.,* 2005; Matano *et al.,* 2014), it was not demonstrated to occur in shelf areas to the north. Such exchange could explain the predominance of the La Plata-sourced clay mineral illite across the shelf surface off southernmost Rio Grande do Sul near Uruguay (Gambôa *et al.,* 1973; Costa & Ramos, 1983). On the other hand, shear zones limit the water and nutrient exchange between the shelf and western boundary currents (Berden *et al.,* 2020), as exemplified by the sharp contrast between the LPP and the BC where mixing is restricted to small vortices (Fig. 7A, B). Although the SW winds that favor the northward intrusion of the LPP were stronger and more frequent during the last glacial as explained above, these would have forced it to flow closer to the shore. Even under conditions of lower sea levels (Fig. 6) it seems unlikely that the plume could have been directed offshore toward the shelf break. Despite the current NE-prevailing winds during summer, which result in offshore movement of the plume through Ekman transport in the south (de Souza & Robinson, 2004; Pimenta *et al.,* 2005; Matano *et al.,* 2014), the plume does not extend beyond the middle shelf along most of the southern Brazilian shelf (Fig. 7A, B). Moreover, geomorphological features (Clapperton, 1993) and sedimentary successions in the upper Paraná River (Stevaux, 2000), the incised paleochannel of the La Plata River (Corrêa *et al.,* 2014) and fossil records and fluvial incisions in the coastal lagoons of Rio Grande do Sul (Lopes *et al.,* 2020b; Barboza *et al.,* 2021b) indicate smaller volume of continental discharges that fed the LPP as a result of drier climate during the last glacial, probably reducing the volume of sediment in the plume and its contribution to ocean productivity.

5.3.3. Upwelling

Another mechanism proposed to explain increases in ocean paleoproductivity off southern Brazil has been upwelling (Pereira *et al.*, 2018, Portilho-Ramos *et al.,* 2019; Bottezini *et al.,* 2022; Suárez-Ibarra *et al.,* 2022). The upwelling results from a combination of pressure gradients related to topography-driven variations of the path of the BC flowing along the shelf break (Fig. 1C) and wind-driven offshore Ekman transport of the surface TW (Palma *et al.,* 2008; Brandini *et al.,* 2014). It is characterized by intrusion up to the middle-inner shelf of the nutrient-rich SACW (Fig. 1C) which is carried southward by the lower layer of the BC at water depths of ~200-500 m (Ciotti *et al.,* 1995; Brandini *et al.,* 2014). Although shelf break upwelling is persistent, the process is increased during summer, when prevailing northeasterly winds push surface shelf waters offshore through Ekman transport, whereas the prevailing southwesterly winds during winter restrict upwelling (Campos *et al.,* 2000; 2013; Palma *et al.,* 2008).

The hypothesis that upwelling could have fueled higher surface productivity farther offshore is hardly reasonable because the nutrient-rich waters of the SACW only reach the lower photic zone over the middle-inner shelf, where it becomes available for photosynthesizing organisms. This process has been demonstrated by seasonal variations recorded north of Rio Grande do Sul (Brandini *et al.,* 2014), where the SACW intrusion reaches shallower depths (~20 m) nearshore during summer, whereas during winter it is restricted to depths >40 meters at the outer-middle shelf. As the SACW provides nutrients that increase productivity only over the shelf, it seems unlikely that it could influence productivity to offshore areas far from the break. Moreover, the stronger, prevailing S-SW winds during the last glacial would have produced conditions analogous to the current winter, thus reducing or precluding upwelling.

5.4. Higher dust inputs to the ocean under future environmental changes

The possibility that wind-blown dust from continental sources across SSA provided nutrients to the adjacent southwestern Atlantic Ocean that favored higher paleoproductivity throughout the Quaternary is relevant not only for the understanding of biogeochemical processes in the past, but also for addressing future effects of dust inputs on oceanic ecosystems that may result from natural and anthropogenically-driven climate and environmental changes.

Different records have shown that dust fluxes during glacial periods were several times higher compared to interglacials (Lamy *et al.,* 2014; Lambert *et al.,* 2015; Albani *et al.,* 2016; Shoenfelt *et al.,* 2018), resulting from higher dust deflation and transport, more notably during stadials such as MIS 4 and 2, related to lower temperatures and weakened hydrologic cycle, among other factors (Yung *et al.,* 1996; Mahowald *et al.,* 1999). It could be expected that the ongoing rise in global temperatures will reduce deflation and entrainment of dust due to the strenghtened hydrological cycle, despite the higher dust availability resulting from the retraction of glaciers (Bullard, 2013). In the case of SSA, however, observations and modeling indicated that certain conditions may arise that could increase the potential for dust deflation and consequently affect surface ocean productivity.

In the last decades, there is a trend of increasing sea surface temperatures (SSTs) in the equatorial Atlantic that affected the patterns of precipitation over South America. This warming caused intensification of the Hadley cell, increasing the ascending movement of air masses in the equatorial zone between summer and autumn, resulting in higher rainfall over the Amazon and stronger air subsidence (higher atmospheric pressure) and thus lower rainfall over subtropical areas located at 10°-40°S (Rao *et al.,* 2016). This process seems to have been a cause of recent droughts in southeastern-southern Brazil and northern-central Argentina (Naumann *et al.,* 2021; Gomes *et al.,* 2021; Rao *et al.,* 2022) and may be a major cause for the increasing loss of ice and lower rainfall in CWA during the last decade (Rivera *et al.,* 2021). It can be hypothesized that if the tendency of more frequent and severe droughts over SSA persists for the next decades as suggested by simulations (Spinoni *et al.,* 2020) this could reduce the vegetation cover and thus increase the extent of the area with dust available for eolian deflation.

Another process that could potentially increase droughts over dust source areas of SSA would be the deforestation of the Amazon rainforest. The evapotranspiration of the rainforest produces large amounts of moisture which are carried from the western Amazon by easterly winds that turn to SE in the form of a low-level jet (LLJ) blowing along the eastern flank of the Andes driven by the Chaco low-pressure area, bringing summer rainfall over southern Brazil, Paraguay, Uruguay, and northern-central Argentina (Satyamurty *et al.,* 1998; Fearnside, 2005; Garreaud *et al.,* 2009). Simulations indicated that the continuing deforestation would result in lower moisture transported southeastwards, thus decreasing summer rainfall across southern Bolivia to northern Argentina (Silva *et al.,* 2016), despite the projected strenghtening of the LLJ under a warmer climate (Soares & Marengo, 2009). On the other hand, a stronger LLJ could increase the deflation and transport of dust from the PAP (Fig. 6). This process may be further increased if El Niño-like conditions, which result in dry conditions over the PAP (Gaiero *et al.,* 2013; Cosentino *et al.,* 2019), become more frequent due to future warming as suggested by some simulations (Latiff & Keenlyside, 2008; Collins *et al.,* 2010).

Both scenarios of continuing ocean warming and deforestation of the Amazon could increase the availability of dust that reaches the southwestern Atlantic Ocean, thus promoting changes in ocean productivity. Under the current scenario of warming oceans, water column stratification will be enhanced, and the reduced vertical mixing will lead to oligotrophic conditions at the surface, thus inhibiting primary productivity (Behrenfeld *et al.,* 2006; Dave & Lozier, 2013; Yamaguchi and Suga, 2019; Li *et al.,* 2020). If episodes of deflated eolian dust reaching the ocean as the ones shown in Figure 1 become more intense due to the higher availability of dust, or more frequent because of changes in atmospheric circulation, this could result in higher ocean productivity. Although such eolian inputs could compensate for the nutrient deficiency, the resulting higher productivity would increase oxygen consumption by respiration of autotroph and heterotroph communities, eventually increasing the O_2-outgassing of the ocean water driven by warmer temperatures (Keeling & Garcia, 2002; Helm *et al.,* 2011), thus leading to dysoxic or anoxic conditions on the ocean surface.

6. Conclusion

Deep sea cores obtained off southern Brazil show variations in the relative proportion of carbonate (biogenic) sand characterized by increases during the last glacial period that exhibit correspondence with intervals of higher dust concentration in ice cores from Antarctica during colder intervals, resulting from a climatic control on the deflation of dust. Because the Antarctic dust was deflated from source areas in SSA (the Puna-Altiplano Plateau, central-western Argentina, and northern Patagonia), that correspondence indicates that dust carried by intensified westerlies and S-SW winds could also have reached the southwestern Atlantic off southern Brazil, therefore providing nutrients that contributed to higher ocean productivity. Deflation processes seem to have been stronger during the stadials MIS 4 and 2 and the late interstadial MIS 3, driven by a combination of 1) equatorward shifted south westerlies belt, 2) expanded glaciers that generated katabatic winds and large amounts of dust, and 3) widespread arid/semiarid conditions with reduced vegetation cover. Dust accumulation in Antarctica was reduced during some of the millennial-scale warming episodes (AIMs). The reduced fluvial discharge and increased eolian deflation related to a drier climate during the last glacial period indicate that wind-supplied dust may have been a major source of nutrients to the adjacent SW Atlantic Ocean, and thus exerted greater influence on ocean paleoproductivity compared to the present.

Although dust-driven increased ocean productivity off SSA was higher during glacial periods, this process still happens today because of dust storms sweeping across the PAP, CWA, and northern Patagonia. Pulses of dust-driven increased productivity may become more frequent in the future due to anthropogenically-induced processes such as modification of atmospheric circulation patterns over South America linked to ocean warming, and deforestation in the Amazon basin, as predicted by some models.

The assessment of the possible influence of glaciogenic dust on the productivity along the southwestern Atlantic is relevant from paleoclimatic and paleoceanographic standpoints because it contributes to the understanding of the climate-driven changes in the landscape, eolian processes, and land-ocean connections during past glacial periods. It can also help to predict future effects on the ocean ecosystems of increased dust inputs that may eventually result from anthropogenically-driven processes such as changes in atmospheric circulation, aridification, and plant cover removal that may happen in the future.

Acknowledgments: The authors would like to thank Dr. Maria Alejandra Gomes Pível (Universidade Federal do Rio Grande do Sul) for providing the sedimentological data from the cores. This research was funded by a postdoctoral grant (Process no. 88887.091728/2014–01) to R.P. Lopes provided by the joint IODP/CAPES (International Ocean Discovery Program/Coordenação de Aperfeiçoamento de Pessoal de Nível Superior) research program. M.S. de Souza is granted with a PNPD-CAPES fellowship (88882.314596/2019-01).

Contribuições dos Autores: Conceptualization, R.P.L. and M.S.S.; methods, R.P.L.; formal analysis, R.P.L. and M.S.S.; research, R.P.L. and M.S.S.; data preparation, R.P.L.; writing, R.P.L.; revision, M.S.S. The authors have read and agree with the published version of the manuscript.

Conflict of Interest: The authors declare no competing interest.

References

Abreu, J.G.N. & Calliari, L.J. 2005. Paleocanais na plataforma continental interna do Rio Grande do Sul: evidências de uma drenagem fluvial pretérita. *Revista Brasileira de Geofísica*, 23(2): 123-132. https://doi.org/10.1590/S0102-261X2005000200002

Albani, S., Mahowald, N.M., Murphy, L.N., Raiswell, R., Moore, J.K., Anderson, R.F., McGee, D., Bradtmiller, L.I., Delmonte, B., Hesse, P.P. & Mayewski, P.A. 2016. Paleodust variability since the Last Glacial Maximum and implications for iron inputs to the ocean. *Geophysical Research Letters*, 43: 3944-3954. https://doi.org/10.1002/2016GL067911.

de Almeida, F.K., de Mello, R.M., Costa, K.B. & Toledo, F.A.L. 2015. The response of deep-water benthic foraminiferal assemblages to changes in paleoproductivity during the Pleistocene (last 769.2 kyr), western South Atlantic Ocean. *Palaeogeography, Palaeoclimatology, Palaeoecology*, 440: 201-212. https://doi.org/10.1016/j.palaeo.2015.09.005

Alves, R.A., da Silva, E.P., Lisniowski M.A., Silva L.G. & Harlamov V. 2021. *Projeto de Prospecção e Exploração de Depósitos de Fosforitas Marinhas na Plataforma Continental Jurídica Brasileira*. CPRM, Rio de Janeiro, 96 p.

Asmus, H.E. & Ponte, F.C. 1973. The Brazilian marginal basins. *In*: Nairn A.E.M. & Stehli F.G. (eds.), *The Ocean Basins and Margins - Volume 1: the South Atlantic*. Springer Science+Business Media, New York, pp. 87-133.

Barboza, E.G., Dillenburg, S.R., Rosa, M.L.C.C., Caron, F., Lopes, R.P., Watanabe, D.S.Z. & Tomazelli, L.J. 2021a. Sistemas deposicionais e evolução geológica da planície costeira entre La Coronilla e Cabo de Santa Marta (Bacia de Pelotas): uma revisão. *In*: Jelinek, A.R. & Sommer, C.A. (eds.), *Contribuições à Geologia do Rio Grande do Sul e de Santa Catarina*. Editora Compasso Lugar Cultura, Porto Alegre, p. 455-468. https://doi.org/10.29327/537860.1-27

Barboza, E.G., Dillenburg, S.R., Lopes, R.P., Rosa, M.L.C.C., Caron, F., Abreu, V., Manzolli, R.P., Nunes, J.C.R., Weschenfelder, J. & Tomazelli, L.J. 2021b. Geomorphological and stratigraphic evolution of a fluvial incision in the coastal plain and inner continental shelf in southern Brazil. *Marine Geology*, 437: 106514. https://doi.org/10.1016/j.margeo.2021.106514

Barker, S. & Diz, P. 2014. Timing of the descent into the last Ice Age determined by the bipolar seesaw. *Paleoceanography*, 29: 489-507. https://doi.org/10.1002/2014PA002623

Basile, I., Grousset, F.E., Revel, M., Petit, J.R., Biscaye, P.E. & Barkov, N.I. 1997. Patagonian origin of glacial dust deposited in East Antarctica (Vostok and Dome C) during glacial stages 2, 4 and 6. *Earth and Planetary Science Letters*, 146(3-4): 573-589. https://doi.org/10.1016/s0012-821x(96)00255-5

Behling, H., Pillar, V.D. & Bauermann, S.G. 2005. Late Quaternary grassland (campos), gallery forest, fire and climate dynamics, studied by pollen, charcoal and multivariate analysis of the São Francisco de Assis core in western Rio Grande do Sul (southern Brazil). *Review of Palaeobotany and Palynology*, 133 (3-4): 235-248. https://doi.org/10.1016/j.revpalbo.2004.10.004

Behrenfeld, M.J., O'Malley, R.T.O., Siegel, D.A., McClain, C.R., Sarmiento, J.L., Feldman, G.C., Milligan, A.J., Falkowski, P.G., Letelier, R.M. & Boss, E.S. 2006. Climate-driven trends in contemporary ocean productivity. *Nature*, 444: 752-755. https://doi.org/10.1038/nature05317

Berden, G., Charo, M., Möller, Jr. O.O. & Piola, A.R. 2020. Circulation and hydrography in the western south atlantic shelf and export to the deep adjacent ocean: 30°S to 40°S. *Journal of Geophysics Research: Oceans*, 125: e2020JC016500. https://doi.org/10.1029/2020JC016500

Bottezini, S.R., Diniz, D., de Ávila, A.S.P. & Leonhardt, A. 2022. Continental influence on the fertilization of marine waters during the late quaternary in the south of the Brazilian continental margin. *Ocean and Coastal Research*, 70: e22021. https://doi.org/10.1590//2675-2824070.21072srb

Brandini, F.P., Nogueira Jr., M., Simião, M., Codina, J.C.U. & Noernberg, M.A. 2014. Deep chlorophyll maximum and plankton community response to oceanic bottom intrusions on the continental shelf in the South Brazilian Bight. *Continental Shelf Research*, 89: 61-75. https://doi.org/10.1016/j.csr.2013.08.002

Bruniard, E.D. 1982. La diagonal árida argentina: un límite climático real. *Revista Geográ*fica, 95: 5-20.

Bullard, J.E. 2013. Contemporary glacigenic inputs to the dust cycle. *Earth Surface Processes and Landforms*, 38(1): 71-89. https://doi.org/10.1002/esp.3315

Butler, L.W. 1970. Shallow structure of the continental margin, southern Brazil and Uruguay. *GSA Bulletin*, 81: 1079-1096. https://doi.org/10.1130/0016-7606(1970)81[1079:SSOTCM]2.0.CO;2

Campos, E.J.D., Lentini, C.A.D., Miller, J.L. & Piola, A.R. 1999. Interannual variability of the sea surface temperature in the South Brazil Bight. *Geophysical Research Letters*, 26(14): 2061-2064. https://doi.org/10.1029/1999GL900297

Campos, E.J.D., Velhote, D. & da Silveira, I.C.A. 2000. Shelf break upwelling driven by Brazil Current cyclonic meanders. *Geophysical Research Letters*, 27(6): 751-754. https://doi.org/10.1029/1999GL010502

Campos, P.C., Möller Jr., O.O., Piola, A.R. & Palma, E.D. 2013. Seasonal variability and coastal upwelling near Cape Santa Marta (Brazil). Jo*urnal of Geophysical Research: Oceans*, 118: 1420-1433. https://doi.org/10.1002/jgrc.20131

Carassai, J.J., Lavina, E.L.C., Chemale Jr., F. & Girelli, T.J. 2019. Provenance of Heavy Minerals for the Quaternary Coastal Plain of Southernmost Brazil (Rio Grande do Sul State) *Journal of Coastal Research*, 35 (2): 295-304. https://doi.org/10.2112/JCOASTRES-D-18-00066.1

Chemale Jr., F., Lavina, E.L.C., Carassai, J.J., Girelli, T.J., & Lana, C. 2021. Andean orogenic signature in the Quaternary sandy barriers of Southernmost Brazilian Passive Margin – Paradigm as a source area. *Geoscience Frontiers*, 12(4): 101119. https://doi.org/10.1016/j.gsf.2020.11.015

Ciotti, Á.M., Odebrecht, C., Fillmann, G. & Möller Jr., O.O. 1995. Freshwater outflow and Subtropical Convergence influence on phytoplankton biomass on the southern Brazilian continental shelf. *Continental Shelf Research*, 15(14): 1737-1756. https://doi.org/10.1016/0278-4343(94)00091-Z

Clapperton, C.M. 1993. *Quaternary Geology and Geomorphology of South America*. Elsevier Press, Amsterdam, 779 p.

Collins M., An S.-I., Cai W., Ganachaud, A., Guilyardi, E., Jin, F., Jochum, M., Lengaigne, M., Power, S., Timmermann, A., Vecchi G. & Wittenberg A. 2010. The impact of global warming on the tropical Pacific Ocean and El Niño. *Nature Geosciences*, 3: 391-397. https://doi.org/10.1038/ngeo868

Corrêa, I.C.S., Medeanic, S., Weschenfelder, J., Toldo Jr., E.E., Nunes, J.C. & Baitelli, R. 2014. The palaeo-drainage of the La Plata River in southern Brazilian shelf. *Revista Brasileira de Geofísica*, 32(2): 259-271. https://doi.org/10.22564/rbgf.v32i2.481

Cosentino, N.J., Gaiero, D.M., Torre, G., Pasquini, A.I., Coppo, R., Arce, J.M. & Vélez, G. 2019. Atmospheric dust dynamics in southern South America: A 14-year modern dust record in the loessic Pampean region. *The Holocene*, 30(4): 575-588. https://doi.org/10.1177/0959683619875198

Costa, C. & Ramos, F.T. 1983. Argilo-minerais na plataforma continental sul-brasileira - do Cabo de Sta. Marta ao Chuí. *Pesquisas em Geociências*, 15: 86-93. https://doi.org/10.22456/1807-9806.21724

Dave, A.C. & Lozier, M.S. 2013. Examining the global record of interannual variability in stratification and marine productivity in the low-latitude and mid-latitude ocean. *Journal of Geophysical Research: Oceans*, 118(6): 2761-3221. https://doi.org/10.1002/jgrc.20224

Dillenburg, S.R. & Barboza, E.G. 2014. The strike-fed sandy coast of Southern Brazil. *In*: Martini I.P. and Wanless H.R. (eds.), *Sedimentary Coastal Zones from High to Low Latitudes: Similarities and Differences*. Geological Society of London, Special Publications vol. 388, p. 333-352. https://doi.org/10.1144/SP388.16.

Dillenburg, S.R., Barboza, E.G., Rosa, M.L.C.C., Caron, F., Cancelli, R., Santos-Fischer, C.B., Lopes, R.P. & Ritter, M.N. 2019. Sedimentary records of Marine Isotopic Stage 3 (MIS 3) in southern Brazil. *Geo-Marine Letters*, 40: 1099-1108. https://doi.org/10.1007/s00367-019-00574-2

Doughty, A.M., Kaplan, M.R., Peltier, C. & Barker, S. 2021. A maximum in global glacier extent during MIS 4. *Quaternary Science Reviews*, 261: 106948. https://doi.org/10.1016/j.quascirev.2021.106948

Dutton, A. & Lambeck, K. 2012. Ice volume and sea level during the last interglacial. *Science*, 337: 216-219. https://doi.org/10.1126/science.1205749

Emilsson, I. 1961. The shelf and coastal waters off southern Brazil. *Boletim do Instituto de Oceanografia*, 11(2): 101-112. https://doi.org/10.1590/S0373-55241961000100004

Fearnside, P.M. 2005. Deforestation in Brazilian Amazonia: history, rates, and consequences. *Conservation Biology*, 19(3): 680-688. https://www.jstor.org/stable/3591054

Frozza, C.F., Pivel, MAG., Suárez-Ibarra, J.Y., Ritter, M.N. & Coimbra, J.C. 2020. Age model of sediment core SAT-048A. *PANGAEA*, https://doi.org/10.1594/PANGAEA.911844,

Gaiero, D.M., Probst, J.-L., Depetris, P.J., Bidart, S.M. & Leleyter, L. 2003. Iron and other transition metals in Patagonian riverborne and windborne materials: Geochemical control and transport to the southern South Atlantic Ocean. *Geochimica et Cosmochimkica Acta*, 67(9): 3603-3623. https://doi.org/10.1016/S0016-7037(03)00211-4

Gaiero, D.M., Simonella, L., Gassó, S., Gili, S., Stein, A.F., Sosa, P., Becchio, R., Arce, J. & Marelli, H. 2013. Ground/satellite observations and atmospheric modeling of dust storms originating in the high Puna-Altiplano deserts (South America): Implications for the interpretation of paleo-climatic archives. *Journal of Geophysical Research: Atmospheres*, 118(9): 3425-3917. https://doi.org/10.1002/jgrd.50036

Gaiero, D.M. 2007. Dust provenance in Antarctic ice during glacial periods: From where in southern South America? *Geophysical Research Letters*, 34: L17707. https://doi.org/10.1029/2007GL030520

García, J.-L., Hein, A.S., Binnie, S.A., Gómez, G.A., González, M.A. & Dunai Tibor, J. 2018. The MIS 3 maximum of the Torres del Paine and Última Esperanza ice lobes in Patagonia and the pacing of southern mountain glaciation. *Quaternary Science Revews*, 185: 9-26. https://doi.org/10.1016/j.quascirev.2018.01.013

Garreaud, R.D., Vuille, M., Compagnucci, R. & Marengo, J. 2009. Present-day South American climate. *Palaeogeography, Palaeoclimatology, Palaeoecology*, 281(3-4): 180-195. https://doi.org/10.1016/j.palaeo.2007.10.032

Gasparini, G.M., Rabassa, J., Deschamps, C. & Tonni, E.P. 2016. *Marine Isotope Stage 3 in Southern South America, 60 Ka BP-30 Ka BP*. Springer International Publishing, Switzerland, 354 p. https://doi.org/10.1007/978-3-319-40000-6.

Gassó, S. & Torres, O. 2019. Temporal Characterization of dust activity in the central Patagonia desert (years 1964–2017). *Journal of Geophysical Research: Atmospheres*, 124: 3417-3434. https://doi.org/10.1029/2018JD030209

Gambôa, L.A.P., Figueiredo Jr., A.G., Martins, I.R. & Formoso, M.L.L. 1973. Argilo-minerais da plataforma continental do Rio Grande do Sul. *In*: Congresso Brasileiro de Geologia, 27, Aracaju. *Anais...*, v. 1: 353-358.

Gili, S., Gaiero, D.M., Goldstein, S.L., Chemale Jr., F., Jweda, J., Kaplan, M.R., Becchio, R.A. & Koester, E. 2017. Glacial/interglacial changes of Southern Hemisphere wind circulation from the geochemistry of South American dust. *Earth and Planetary Science Letters*, 469: 98–109. https://doi.org/10.1016/j.epsl.2017.04.007

Gomes, M.S., Cavalcanti, I.F.A. & Müller, G.V. 2021. 2019/2020 drought impacts on South America and atmospheric and oceanic influences. *Weather and Climate Extremes*, 34: 100404. https://doi.org/10.1016/j.wace.2021.100404

Gonçalves, J.F. & Leonhardt, A. 2021. A influência dos processos de fundo sobre um registro fóssil de cocolitoforídeos na Bacia de Pelotas. *Anais do Instituto de Geociências*, 44: 36784. https://doi.org/10.11137/1982-3908_2021_44_36784

González-Silvera, A., Santamaria-del-Angel, E. & Millán-Núñez, R. 2006. Spatial and temporal variability of the Brazil-Malvinas Confluence and the La Plata Plume as seen by SeaWiFS and AVHRR imagery. *Journal of Geophysical Research*, 111: C06010. https://doi.org/10.1029/2004JC002745

Grant, K.M., Rohling, E.J., Bar-Matthews, M., Ayalon, A., Medina-Elizalde, M., Ramsey, C.B., Satow, C. & Roberts, A.P. 2012. Rapid coupling between ice volume and polar temperature over the past 150,000 years. *Nature*, 491: 744–747. https://doi.org/10.1038/nature11593

Gu, F., Zonneveld, K.A.F., Chiessi, C.M., Arz, H.W., Pätzold, J. & Behling, H. 2017 Long-term vegetation, climate and ocean dynamics inferred from a 73,500 years old marine sediment core (GeoB2107-3) off southern Brazil. *Quaternary Science Reviews*, 172: 55-71. https://doi.org/10.1016/j.quascirev.2017.06.028

Gu, F., Chessi, C.M., Zonneveld, K.A.F. & Behling, H. 2019. Shifts of the Brazil-Falklands/Malvinas Confluence in the western South Atlantic during the latest Pleistocene–Holocene inferred from dinoflagellate cysts. *Palynology*, 43(3): 483-493. https://doi.org/10.1080/01916122.2018.1470116

Hearty, P.J., Hollin, J.T., Neumann, A.C., O'Leary, M.J. & McCulloch, M. 2007. Global sea-level fluctuations during the last interglacial (MIS 5e). *Quaternary Science Reviews*, 26(17-18): 2090-2112. https://doi.org/10.1016/j.quascirev.2007.06.019

Helm, K.P., Bindoff, N.L. & Church, J.A. 2011. Observed decreases in oxygen content of the global ocean. *Geophysical Research Letters*, 38(23): L23602. https://doi.org/10.1029/2011GL049513

Heusser, C.J. 1974. Vegetation and climate of the southern Chilean lake district during and since the last interglaciation. *Quaternary Research*, 4(3): 290-315. https://doi.org/10.1016/0033-5894(74)90018-0

Heusser, C.J. 1989. Southern westerlies during the Last Glacial Maximum. *Quaternary Research*, 31(3): 423-425. https://doi.org/10.1016/0033-5894(89)90049-5

Heusser, L., Heusser, C., Mix, A.& McManus, J. 2006. Chilean and Southeast Pacific paleoclimate variations during the last glacial cycle: directly correlated pollen and $\delta^{18}O$ records from ODP Site 1234. *Quaternary Science Reviews*, 25(23-24): 3404-3415. https://doi.org/10.1016/j.quascirev.2006.03.011

Hulton, N, Sugden, D, Payne, A. & Clapperton, C. 1994. Glacier modeling and the climate of Patagonia during the Last Glacial Maximum. *Quaternary Research*, 42(1): 1-19. https://doi.org/10.1006/qres.1994.1049

Iriondo, M.H. 1997. Models of deposition of loess and loessoids in the Upper Quaternary of South America. *Journal of South American Earth Sciences*, 10(1): 71-79. https://doi.org/10.1016/S0895-9811(97)00006-0

Iriondo, M.H. 1999. Last Glacial Maximum and Hypsithermal in the Southern Hemisphere. *Quaternary International*, 62(1): 11-19. https://doi.org/10.1016/s1040-6182(99)00019-1

Iriondo, M.H. 2000. Patagonian dust in Antarctica. *Quaternary International*, 68-71: 83-86. https://doi.org/10.1016/s1040-6182(00)00035-5

Iriondo, M.H. & Kröhling, D.M. 1995. El Sistema Eólico Pampeano. *Comunicaciones del Museo Provincial de Ciencias Naturales "Florentino Ameghino*", 5(1): 1-68.

Johnson, M.J., Meskhidze, N., Kiliyanpilakkil, V.P. & Gassó, S. 2011. Understanding the transport of Patagonian dust and its influence on marine biological activity in the South Atlantic Ocean. *Atmospheric Chemistry and Physics*, 11: 2487-2502. https://doi.org/10.5194/acp-11-2487-2011

Kaiser, J. & Lamy, F. 2010. Links between Patagonian Ice Sheet fluctuations and Antarctic dust variability during the last glacial period (MIS 4-2). *Quaternary Science Reviews*, 29: 1464-1471. https://doi.org/10.1016/j.quascirev.2010.03.005

Kaiser, J., Lamy, F. & Hebbeln, D. 2005. A 70-kyr sea surface temperature record off southern Chile (Ocean Drilling Program Site 1233). *Palaeoceanography*, 20: PA4009. https://doi.org/10.1029/2005PA001146

Keeling, R.F. & Garcia, H.E. 2002. The change in oceanic O_2 inventory associated with recent global warming. *Proceedings of the National Academy of Sciences*, 99(12): 7848-7853. https://doi.org/10.1073/pnas.122154899

Kowsmann, R.O., Costa, M.P.A., Vicalvi, M.A., Coutinho, M.G.N. & Gambôa, L.A.P. 1977. *Modelo da sedimentação holocênica na plataforma continental sul brasileira*. Rio de Janeiro, PETROBRÁS, Projeto REMAC, v.2, p. 7-26.

Kumar, N., Anderson, R.F., Mortlock, R.A., Froelich, P.N., Kubik, P., Dittrich-Hannen, B. & Suter, M. 1995. Increased biological productivity and export production in the glacial Southern Ocean. *Nature*, 378: 675-680. https://doi.org/10.1038/378675a0

Lambert, F., Delmonte, B., Petit, J.R., Bigler, M., Kaufmann, P.R., Hutterli, M.A., Stocker, T.F., Ruth, U., Steffensen, J.P. & Maggi, V. 2008. Dust-climate couplings over the past 800,000 years from the EPICA Dome C ice core. *Nature* 452: 616-619. https://doi.org/10.1038/nature06763

Lambert, F., Bigler, M., Steffensen, J.P., Hutterli, M. & Fischer, H. 2012. Centennial mineral dust variability in high-resolution ice core data from Dome C, Antarctica. *Climate of the Past*, 8: 609-623. https://doi.org/10.5194/cp-8-609-2012

Lambert, F., Tagliabue, A., Shaffer, G., Lamy, F., Winckler, G., Farias, L., Gallardo, L. & De Pol-Holz, R. 2015. Dust fluxes and iron fertilization in Holocene and Last Glacial Maximum climates. *Geophysical Research Letters*, 42: 6014-6023. https://doi.org/10.1002/2015GL064250

Lamy, F., Hebbeln, D. & Wefer, G. 1998. Late Quaternary precessional cycles of terrigenous sediment input off the Norte Chico, Chile (27.5°S) and palaeoclimatic implications. *Palaeogeography, Palaeoclimatology, Palaeoecology*, 141(3-4): 233-251. https://doi.org/10.1016/S0031-0182(98)90052-9

Lamy, F., Gersonde, R., Winckler, G., Esper, O., Jaeschke, A., Kuhn, G., Ullermann, J., Martínez-Garcia, A., Lambert, F. & Kilian, R. 2014. Increased dust deposition in the Pacific southern ocean during glacial periods. *Science*, 343: 403-407. https://doi.org/10.1126/science.1245424

Lantszch, H., Hanebuth, T.J.J., Chiessi, C.M., Schwenk, T. & Violante, R.A. 2014. The high-supply, current-dominated continental margin of southeastern South America during the late Quaternary. *Quaternary Research*, 81: 339-354. https://doi.org/10.1016/j.yqres.2014.01.003

Laprida, C., Chapori, N.G., Chiessi, C.M., Violante, R.A., Watanabe, S. & Totah, V. 2011. Middle Pleistocene sea surface temperature in the Brazil-Malvinas Confluence Zone: Paleoceanographic implications based on planktonic foraminifera. *Micropaleontology*, 57(2): p. 183-194. https://www.jstor.org/stable/41410980

Latif, M. & Keenlyside, N.S. 2008. El Niño/Southern Oscillation response to global warming. *Proceedings of the National Academy of Sciences*, 106(49): 20578-20583. https://doi.org/10.1073pnas.0710860105

Ledru, M.-P., Braga, P.I.S., Soubiès, F., Fournier, M., Martin, L., Suguio, K. & Turcq, B. 1996. The last 50,000 years in the Neotropics (Southern Brazil): evolution of vegetation and climate. *Palaeogeography, Palaeoclimatology, Palaeoecology*, 123(1-4): 239-257. https://doi.org/10.1016/0031-0182(96)00105-8

Ledru, M.-P., Cordeiro, R.C., Dominguez, J.M.L., Martin, L., Mourguiart, P. & Sifeddine, A. 2001. Late-glacial cooling in Amazonia inferred from pollen at Lagoa do Caçó, northern Brazil. *Quaternary Research*, 55(1): 47-56. https://doi.org/10.1006/qres.2000.2187

Li, G., Cheng, L., Zhu, J., Trenberth, K.E., Mann, M.E. & Abraham, J.P. 2020. Increasing ocean stratification over the past half-century. *Nature Climate Change*, 10: 1116-1123. https://doi.org/10.1038/s41558-020-00918-2

Lima, S.F., Almeida, L.E. & Toldo Jr., E.E. 2001. Estimativa da capacidade de transporte longitudinal de sedimentos a partir de dados de ondas para a costa do Rio Grande do Sul. *Pesquisas em Geociências*, 28(2): 99-107. https://doi.org/10.22456/1807-9806.20272

Lisiecki, L.E. & Raymo, M.E. 2005. A Pliocene-Pleistocene stack of 57 globally distributed benthic $\delta^{18}O$ records. *Paleoceanography*, 20: PA1003. https://doi.org/10.1029/2004PA001071

Lisniowski, M.A. & Alves, R.A. 2018a. *Mapa de retroespalhamento acústico do Terraço do Rio Grande (Escala 1:250.000)*. CPRM, Rio de Janeiro. http://rigeo.cprm.gov.br/jspui/handle/doc/20429.

Lisniowski, M.A. & Alves, R.A. 2018b. *Mapa Batimétrico do Terraço do Rio Grande - Escala 1:250.000)*. CPRM, Rio de Janeiro. http://rigeo.cprm.gov.br/jspui/handle/doc/20428.

Lopes, R.P., Dillenburg, S.R. & Schultz, C.L. 2016a. Cordão Formation: loess deposits in the southern coastal plain of the state of Rio Grande do Sul. Brazil. *Anais da Academia Brasileira de Ciências*, 88(4): 2143-2166. https://doi.org/10.1590/0001-3765201620150738

Lopes, R.P., Dillenburg, S.R., Sial, A.N., Guadagnin, F. & Caron, F. 2016a. The Caliche Cordão of the southern coastal plain of Rio Grande do Sul, Brazil. *In*: Congresso Brasileiro de Geologia, 48, 2016, Porto Alegre. *Anais*: http://cbg2017anais.siteoficial.ws/sts/st29.htm

Lopes, R.P., Pereira, J.C., Kinoshita, A., Mollemberg, M., Barbosa Jr., F., & Baffa, O. 2020a. Geological and taphonomic significance of electron spin resonance (ESR) ages of Middle-Late Pleistocene marine shells from barrier-lagoon systems of Southern Brazil. *Journal of South American Earth Sciences*, 101: 102605. https://doi.org/10.1016/j.jsames.2020.102605

Lopes, R.P., Pereira, J.C., Dillenburg, S.R., Tatumi, S.H., Yee, M., Figueiredo, A.M.G., Kinoshita, A. & Baffa, O. 2020b. Late Pleistocene-Holocene fossils from Mirim Lake, southern Brazil, and their paleoenvironmental significance: I - vertebrates. *Journal of South American Earth Sciences*, 100: 102566. https://doi.org/10.1016/j.jsames.2020.102566

Lopes, R.P., Bonetti, C., Santos, G.S., Pivel, M.A.G., Petró, S., Caron, F. & Bonetti, J. 2021a. Late Pleistocene sediment accumulation in the lower slope off the Rio Grande terrace, southern Brazilian Continental Margin. *Quaternary International*, 571: 97-116. https://doi.org/10.1016/j.quaint.2020.12.022

Lopes, R.P., Dillenburg, S.R., Savian, J.F. & Corrêa, J.C. 2021b. The Santa Vitória Alloformation: an update on a Pleistocene fossil-rich unit in Southern Brazil. *Brazilian Journal of Geology*, 51(1): e2020065. https://doi.org/10.1590/2317-4889202120200065

Lopes, R.P., Scherer, C.S., Pereira, J.C. & Dillenburg, S.R. 2023. Paleoenvironmental changes in the Brazilian Pampa based on carbon and oxygen stable isotope analysis of Pleistocene camelid tooth enamel. *Journal of Quaternary Sciences*, 38(5): 702-718. https://doi.org/10.1002/jqs.3502

Maher, B.A., Prospero, J.M., Mackie, D., Gaiero, D.M., Hesse, P.P. & Balkanski, Y. 2010. Global connections between aeolian dust, climate and ocean biogeochemistry at the present day and at the last glacial maximum. *Earth-Science Reviews*, 99(1-2): 61-97. https://doi.org/10.1016/j.earscirev.2009.12.001

Mahowald, N., Kohfeld, K., Hansson, M., Balkanski, Y., Harrison, S.P., Prentice, I.C., Schulz, M. & Rodhe, H. 1999. Dust sources and deposition during the last glacial maximum and current climate: A comparison of model results with paleodata from ice cores and marine sediments. *Journal of Geophysical Research*, 104(D13): 15895-15916. https://doi.org/10.1029/1999JD900084

Martin, J.H. 1990. Glacial-interglacial CO_2 change: The Iron Hypothesis. *Paleoceanography and Paleoclimatology*, 5(1): 1-13. https://doi.org/10.1029/PA005i001p00001

Martínez-García, A., Rosell-Melé, A., Jaccard, S.L., Geibert, W., Sigman, D.M. & Haug, G.H. 2011. Southern Ocean dust–climate coupling over the past four million years. *Nature*, 476: 312-316. https://doi.org/10.1038/nature10310

Martínez-García, A., Sigman, D.M., Ren, H., Anderson, R.F., Straub, M., Hodell, D.A., Jaccard, S.L., Eglinton, T.I. & Haug, G.H. 2014. Iron fertilization of the subantarctic ocean during the last ice age. *Science*, 343: 1347-1350. https://doi.org/10.1126/science.1246848

Matano, R.P., Schlax, M.G. & Chelton, D.B. 1993. Seasonal variability in the southwestern Atlantic. *Journal of Geophysical Research*, 98(C10): 18027-18035. https://doi.org/10.1029/93jc01602

Matano, R.P., Combes, V., Piola, A.R. *et al.* 2014. The salinity signature of the cross-shelf exchanges in the Southwestern Atlantic Ocean: numerical simulations. *Journal of Geophysical Research: Oceans*, 119(1): 7949-7968. https://doi.org/10.1002/2014JC010113

Mohtadi, M. & Hebbeln, D. 2004. Mechanisms and variations of the paleoproductivity off northern Chile (24°S–33°S) during the last 40,000 years, *Paleoceanography*, 19: PA2023. https://doi.org/10.1029/2004PA001003

Mourelle, D., del Puerto, L., Pérez, L., Bergamino, L. & García-Rodríguez, F. 2020. Late Pleistocene and Late Holocene environment and climate in the campos region of southeastern South America inferred from phytolith, diatom and geochemical data. *Palaeogeography, Palaeoclimatology, Palaeoecology*, 543:109586. https://doi.org/10.1016/j.palaeo.2020.109586.

Naumann, G., Podestá, G., Marengo, J., Luterbacher, J., Bavera, D., Arias Muñoz, C., Barbosa, P., Cammalleri, C., Chamorro, L., Cuartas, A., de Jager, A., Escobar, C., Hidalgo, C., Leal de Moraes, O., McCormick N., Maetens, W., Magni, D., Masante, D., Mazzeschi, M., Seluchi, M., Skansi, M. M., Spinoni, J. & Toreti., A. 2021. *The 2019-2021 extreme drought episode in La Plata Basin*. EUR 30833 EN, Publications Office of the European Union, Luxembourg, 2021, ISBN 978-92-76-41898-6. https://doi.org/10.2760/773.

Noble, T.L., Piotrowski, A.M., Robinson, L.F., McManus, J.F., Hillenbrand, C.-D. & Bory, A.J.-M. 2012. Greater supply of Patagonian-sourced detritus and transport by the ACC to the Atlantic sector of the Southern Ocean during the last glacial period. *Earth and Planetary Science Letters*, 317-318: 374–385. https://doi.org/10.1016/j.epsl.2011.10.007

Palma, E.D., Matano, R.P. & Piola, A.R. 2008. A numerical study of the Southwestern Atlantic shelf circulation: Stratified Ocean response to local and offshore forcing. *Journal of Geophysical Research*, 113: C11010. https://doi.org/10.1029/2007JC004720

Panario, D. & Gutiérrez, O. 1999. The continental Uruguayan Cenozoic: an overview. *Quaternary International*, 62(1): 75-84. https://doi.org/10.1016/S1040-6182(99)00025-7

Paparazzo, F.E., Crespi-Abril, A.C., Gonçalves, R.J., Barbieri, E.S., Gracia Villalobos, L.L., Solís, M.E. & Soria, G. 2018. Patagonian dust as a source of macronutrients in the Southwest Atlantic Ocean. *Oceanography*, 31(4): 33-39. https://doi.org/10.5670/oceanog.2018.408.

Parrenin, F., Barnola, J.-M., Beer, J., Blunier, T., Castellano, E., Chappellaz, J., Dreyfus, G., Fischer, H., Fujita, S., Jouzel, J., Kawamura, K., Lemieux-Dudon, B., Loulergue, L., Masson-Delmotte, V., Narcisi, B., Petit, J.-R., Raisbeck, G., Raynaud, D., Ruth, U., Schwander, J., Severi, M., Spahni, R., Steffensen, J.P., Svensson, A., Udisti, R., Waelbroeck, C. & E. Wolff 2007. The EDC3 chronology for the EPICA Dome C ice core. *Climate of the Past*, 3: 485-497. https://doi.org/10.5194/cp-3-485-2007

Peltier, C., Kaplan, M.R., Birkel, S.D., Soteres, R.L., Sagredo, E.A., Aravena, J.C., Araos, J., Moreno, P.I., Schwartz, R. & Schaefer, J.M. 2021. The large MIS 4 and long MIS 2 glacier maxima on the southern tip of South America. *Quaternary Science Reviews*, 262: 106858. https://doi.org/10.1016/j.quascirev.2021.106858

Pereira, C.S. 1989. Seasonal variability in the coastal circulation on the Brazilian continental shelf (29°S-35°S). *Continental Shelf Research*, 9(3): 285-299. https://doi.org/10.1016/0278-4343(89)90029-0

Pereira, L.S., Arz, H.W., Pätzold, J. & Portilho-Ramos, R.C. 2018. Productivity evolution in the south Brazilian bight during the last 40,000 years. *Paleoceanography and Paleoclimatology*, 33(12): 1339-1356. https://doi.org/10.1029/2018PA003406

Petró, S.M. 2018. *Dissolução de Foraminíferos Quaternários do Atlântico Sul: da perda de* $CaCO_3$ *ao ganho de informação paleoceanográfica*. PhD Thesis. Universidade Federal do Rio Grande do Sul, Programa de Pós-graduação em Geociências, 146 p. http://hdl.handle.net/10183/174078

Petró, S.M., Pivel, M.A.G. & Coimbra, J.C. 2021. Evidence of supra-lysoclinal dissolution of pelagic calcium carbonate in the late Quaternary in the western South Atlantic. *Marine Micropaleontology*, 166: 102013. https://doi.org/10.1016/j.marmicro.2021.102013

Pico, T., Mitrovica, J.X., Ferier, K.L. & Braun, J. 2016. Global ice volume during MIS 3 inferred from a sea-level analysis of sedimentary core records in the Yellow River Delta. *Quaternary Science Reviews*, 152: 72-79. https://doi.org/10.1016/j.quascirev.2016.09.012

Pimenta, F.M., Campos, E.J.D., Miller, J.L. & Piola, A.R. 2005. A numerical study of the La Plata River plume along the southeastern South American continental shelf. *Brazilian Journal of Oceanography*, 53(3/4): 129-146.

Piola, A.R., Campos, E.J.D., Môller Jr., O.O., Charo, M. & Martinez, C. 2000. Subtropical shelf front off eastern South America. *Journal of Geophysical Research*, 105(C3): 6565-6578. https://doi.org/10.1029/1999JC000300

Piola, A.R., Matano, R.P., Palma, E.D., Môller Jr., O.O. & Campos, E.J.D. 2005. The influence of the Plata River discharge on the western South Atlantic shelf. *Geophysical Research Letters*, 32: L01603. https://doi.org/10.1029/2004GL021638

Piola, A.R. & Matano, R.P. 2009. Brazil and Falklands (Malvinas) currents. *In*: Steele J.H., Thorpe S.A., Turekian K.K. (eds.), *Encyclopedia of Ocean Sciences* (2nd ed.), v.1, p. 422-430.

Portilho-Ramos, R.C., Pinho, T.M.L., Chiessi, C.M. & Barbosa, C.F. 2019. Understanding the mechanisms behind high glacial productivity in the southern Brazilian margin. *Climate of the Past*, 15(3): 943-955. https://doi.org/10.5194/cp-15-943-2019

Potter, E.-K., Esat, T.M., Schellmann, G., Radtke, U., Lambeck, K. & McCulloch, M.T. 2004. Suborbital-period sea-level oscillations during marine isotope substages 5a and 5c. *Earth and Planetary Science Letters*, 225: 191-204. https://doi.org/10.1016/j.epsl.2004.05.034

Prieto, A.R. 1996. Late Quaternary vegetational and climatic changes in the Pampa grassland of Argentina. *Quaternary Research*, 45(1): 73-88. https://doi.org/10.1006/qres.1996.0007

Prospero, J.M., Ginoux, P., Torres, O., Nicholson, S.E. & Gill, T.E. 2002. Environmental characterization of global sources of atmospheric soil dust. *Reviews of. Geophysics*, 40(1): 1002. https://doi.org/10.1029/2000RG000095

Quattrochio, M.E. & Borromei, A.M. 1998. Paleovegetational and paleoclimatic changes during the late Quaternary in southwestern Buenos Aires Province and southern Tierra Del Fuego (Argentina). *Palynology*, 22(1): 67-82.

Rabineau, M., Berné, S., Olivet, J.-L., Aslanian, D., Guillocheau, F. & Joseph, P. 2006. Paleo sea levels reconsidered from direct observation of paleoshoreline position during Glacial Maxima (for the last 500,000 yr). *Earth and Planetary Science Letters*, 252(1–2): 119-137. https://doi.org/10.1016/j.epsl.2006.09.033

Railsback, L.B., Gibbard, P.L., Head, M.J., Voarintsoa, N.R.G. & Taucanne, S. 2015. An optimized scheme of lettered marine isotope substages for the last 1.0 million years, and the climatostratigraphic nature of isotope stages and substages. *Quaternary Science Reviews*, 111: 94-106. https://doi.org/10.1016/j.quascirev.2015.01.012

Rao, V.B., Franchito, S.H., Santo, C.M.E. & Gan, M.A. 2016. An update on the rainfall characteristics of Brazil: seasonal variations and trends in 1979–2011. *International Journal of Climatology*, 36: 291-302. https://doi.org/10.1002/joc.4345

Rao, V.B., Franchito, S.H., Rosa, M.B., Govardhan, D., Figueroa, S.N. & Bhargavi, V.S.L. 2022. In a changing climate Hadley cell induces a record flood in amazon and another recorded drought across South Brazil in 2021. *Natural Hazards*, 114: 1549-1561. https://doi.org/10.1007/s11069-022-05437-1

Reid, J.R., Nowlin Jr., W.D. & Patzert, W.C. 1977. On the characteristics and circulation of the southwesterm Atlantic Ocean. *Journal of Physical Oceanography*, 7: 62-91. https://doi.org/10.1175/1520-0485(1977)007<0062:OTCACO>2.0.CO;2

Rivera, J.A., Otta, S., Lauro, C. & Zazulle, N. 2021. A decade of hydrological drought in central-western Argentina. *Frontiers in Water*, 3: 640544. https://doi.org/10.3389/frwa.2021.640544

Rodrigues, A.R., Pivel, M.A.G., Schmitt, P., de Almeida, F.K. & Bonetti, C. 2018. Infaunal and epifaunal benthic foraminifera species as proxies of organic matter paleofluxes in the Pelotas Basin, south-western Atlantic Ocean. *Marine Micropaleontology*, 144: 38-49. https://doi.org/10.1016/j.marmicro.2018.05.00

Rohling ,E.J., Fenton, M., Jorissen, F.J., Bertrand, P., Ganssen, G. & Caulet, J.P. 1998. Magnitudes of sea-level lowstands of the past 500,000 years. *Nature*, 394: 162-165. https://doi.org/10.1038/28134.

Satyamurty, P., Nobre, C.A. & Dias, P.L.S. 1998. South America. *In*: Koroly D.J. and Vincent D.G. (eds.), *Meteorology of the Southern Hemisphere*. Meteorological Monographs, 27(49): 119-139.

Schaefer, J.M., Putnam, A.E., Denton, G.H., Kaplan, M.R., Birkel, S., Doughty, A.M., Kelley, S., Barrell, D.J.A., Finkel, R.C., Winckler, G., Anderson, R.F., Ninneman, U.S., Barker, S., Schwartz, R., Andersen, B.G. & Schluechter, C. 2015. The southern glacial maximum 65,000 years ago and its unfinished termination. *Quaternary Science Reviews*, 114: 52-60. https://doi.org/10.1016/j.quascirev.2015.02.009

Schmitt, P., Rodrigues, A.R. & Bonetti, C. 2019. Sucessão de associações de foraminíferos bentônicos como indicadoras de variações paleoceanográficas no terraço de Torres (RS-Brasil) durante o Quaternário. *Anuário do Instituto de Geociências*, 42(4): 387-395. https://doi.org/10.11137/2019_4_387_395

Shoenfelt, E.M., Winckler, G., Lamy, F., Anderson, R.F. & Bostick, B.C. 2018. Highly bioavailable dust-borne iron delivered to the Southern Ocean during glacial periods. *Proceedings of the National Academy of Sciences*, 115(44): 11180-11185. https://doi.org/10.1073/pnas.1809755115

Silva, M.E.S., Pereira, G. & da Rocha, R.P. 2016. Local and remote climatic impacts due to land use degradation in the Amazon “Arc of Deforestation”. *Theoretical and Applied Climatology*, 125: 609-623. https://doi.org/10.1007/s00704-015-1516-9

Soares, W.R. & Marengo, J.A. 2009. Assessments of moisture fluxes east of the Andes in South America in a global warming scenario. *International Journal of Climatology*, 29: 1395-1414. https://doi.org/10.1002/joc.1800

de Souza, R.B. & Robinson, I.R. 2004. Lagrangian and satellite observations of the Brazilian Coastal Current. *Continental Shelf Research*, 24: 241-262. https://doi.org/10.1016/j.csr.2003.10.001

Spinoni, J., Barbosa, P., Bucchignani, E. *et al.* 2020. Future global meteorological drought hot spots: a study based on CORDEX data. *Journal of Climatology*, 33: 3635-3661. https://doi.org/10.1175/JCLI-D-19-0084.1

Stevaux, J.C. 2000. Climatic events during the late Pleistocene and Holocene in the upper Paraná River: Correlation with NE Argentina and South-Central Brazil. *Quaternary International*, 72(1): 73-85. https://doi.org/10.1016/S1040-6182(00)00023-9

Stramma, L. & England, M. 1999. On the water masses and mean circulation of the South Atlantic Ocean. *Journal of Geophyical Research: Oceans*, 104(C9): 20863-20883. https://doi.org/10.1029/1999jc900139

Suárez-Ibarra, J.Y., Frozza, C.F., Palhano, P.L., Petró, S.M., Weinkauf, M.F.G. & Pivel, M.A.G. 2022. Calcium carbonate dissolution triggered by high productivity during the last glacial–interglacial interval in the deep western South Atlantic. *Frontiers in Earth Sciences*, 10: 830984. https://doi.org/10.3389/feart.2022.830984

Sugden, D.E., McCulloch, R.D., Bory, A.J.-M. & Hein, A.S. 2009. Influence of Patagonian glaciers on Antarctic dust deposition during the last glacial period. *Nature Geosciences*, 2: 281-285. https://doi.org/10.1038/NGEO474

Sun, X., Corliss, B.H., Brown, C.W. & Shower, W.J. 2006. The effect of primary productivity and seasonality on the distribution of deep sea benthic foraminifera in the North Atlantic. *Deep Sea Research, Part I*, 53(1): 28-47. https://doi.org/10.1016/j.d sr.2005.07.003

Thomas, E. & Gooday, A.J. 1996. Cenozoic deep-sea benthic foraminifers: Tracers for changes in oceanic productivity? *Geology*, 24(4): 355-358. https://doi.org/10.1130/0091-7613(1996)024<0355:cdsbft>2.3.co

Thomas, E., Booth, L., Maslin, M. & Shackleton, N.J. 1995. Northeastern Atlantic benthic foraminifera during the last 45,000 years: Changes in productivity seen from the bottom up. *Paleoceanography and Paleoclimatology*, 10(3): 545-562. https://doi.org/10.1029/94PA03056

Tonello, M.S. & Prieto, A.R. 2010. Tendencias climáticas para los pastizales pampeanos durante el Pleistoceno tardío-Holoceno: estimaciones cuantitativas basadas en secuencias polínicas fósiles. *Ameghiniana*, 47(4): 501-514.

Torre, G., Gaiero, D.M., Sawakuchi, A.O., del Río, I. & Coppo, R. 2019. Revisiting the chronology and environmental conditions for the accretion of late Pleistocene-early Holocene Pampean loess (Argentina). *Quaternary Science Reviews*, 213: 105-119. https://doi.org/10.1016/j.quascirev.2019.04.018

Torre, G., Gaiero, D.M., Coppo, R., Cosentino, N., Goldstein, S., De Vleeschouwer, F., Le Roux, G., Bolge, L., Kiro, Y. & Sawakuchi, A.O. 2022. Unraveling late Quaternary atmospheric circulation in the Southern Hemisphere through the provenance of Pampean loess. *Earth-Science Reviews*, 232: 104143. https://doi.org/10.1016/j.earscirev.2022.104143

van den Heuvel, E.P.J. 1966. On the precession as a cause of Pleistocene variations of the Atlantic Ocean water temperatures. *Geophysical Journal International*, 11(3): 323-336. https://doi.org/10.1111/j.1365-246X.1966.tb03086.x

Villwock, J.A. & Tomazelli, L.J. 1995. Geologia Costeira do Rio Grande do Sul. *Notas Técnicas*, 8: 1-45.

Voelker, A.H.L. 2002. Global distribution of centennial-scale records for Marine Isotope Stage (MIS) 3: a database. *Quaternary Science Reviews*, 21(10): 1185–1212. https://doi.org/10.1016/s0277-3791(01)00139-1

Weber, M.E., Kuhn, G., Sprenk, D., Rolf, C., Ohlwein, C. & Ricken, W. 2012. Dust transport from Patagonia to Antarctica e A new stratigraphic approach from the Scotia Sea and its implications for the last glacial cycle. *Quaternary Science Reviews*, 36: 177-188. https://doi.org/10.1016/j.quascirev.2012.01.016

Williams, G.E. 1993. History of the Earth's obliquity. *Earth-Science Reviews*, 34: 1-45.

Yamaguchi, R. & Suga, T. 2019. Trend and variability in global upper-ocean stratification since the 1960s. *Journal of Geophysical Research: Oceans*, 124: 8933-8948. https://doi.org/10.1029/2019JC015439

Yung, Y.L., Lee, T., Wang, C.-H. & Shieh, Y.-T. 1996. Dust: A Diagnostic of the Hydrologic Cycle During the Last Glacial Maximum. *Science*, 271: 962-963. https://doi.org/10.1126/science.271.5251.9

Zárate, M.A. 2006. Loess Records/South America. *In*: Elias, S.A. (ed.), *Encyclopedia of Quaternary Science*. Elsevier Science, Amsterdam, p. 1466-1479.

Zárate, M.A. & Tripaldi, A. 2012. The aeolian system of central Argentina. *Aeolian Research*, 3(4): 401-417.https://doi.org/10.1016/j.aeolia.2011.08.002

Zárate, M.A., Mehl, A. & Tripaldi, A. 2016. The Continental Record of Marine Isotope Stage 3 (MIS 3; ~60–25 ka) in Central Argentina: Evidence from Fluvial and Aeolian Sequences. *In*: Gasparini, G.M., Rabassa, J., Deschamps, C. & Tonni, E.P. (eds.), *Marine Isotope Stage 3 in Southern South America, 60 Ka BP-30 Ka BP*. Springer International Publishing, Switzerland, p. 167-181. https://doi.org/10.1007/978-3-319-40000-6_10

Zech, R., Zech, J., Kull, Ch., Kubik, P.W. & Veit, H. 2011. Early last glacial maximum in the southern Central Andes reveals northward shift of the westerlies at ~39 ka. *Climate of the Past*, 7: 41-46. https://doi.org/10.5194/cp-7-41-2011

Zembruscki, S.G. 1979. *Geomorfologia da margem continental sul brasileira e da bacia oceânica adjacente*. Rio de Janeiro, PETROBRÁS, Projeto REMAC, v.7, p. 129-177.